Quantifying Climate Risk Premia

Lionel Melin* Fangyuan Zhang†

December 19, 2025

Abstract

What are the quantified risks that climate change poses for financial markets? The physics of climate change are well understood with their uncertainty. Empirical studies provide estimates of the economic damage from rising global temperatures and the costs of curbing such a rise. We build on this basis a precisely calibrated dual framework: linking a climate module with a long-run-risks workhorse asset-pricing model. It incorporates both physical damage and transition cost channels, while capturing the economic activity impact on temperatures. Our framework delivers closed-form solutions for climate-affected and time-dependent risk-free rate, equity risk premia and price-dividends ratios. We show that chronic climate risks alone, away from tipping points, result in an increase of the equity risk premium by almost 20% in a 3°C world. Enough to anticipate a likely market repricing.

Keywords: Climate Risks, Physical Damages and Transition Costs, Asset Pricing, Long-Run-Risks Model, Equity Risk Premium

JEL classification: G11, G12, G51, G54

*EDHEC Climate Institute, MacroLucid Research, Email: lionel.melin@climateimpactedhec.com

†EDHEC Climate Institute, EDHEC Business School, Email: fangyuan.zhang@climateimpactedhec.com

1 Introduction

How does global warming impact risks priced by markets? To address this question, we propose a framework that ties together a workhorse of macro-finance, the long-run risks (LRR) model, together with a physical climate module, which captures a wide range of alternative climate scenarios. We calibrate the full framework, first working on each of the modules separately, and then linking them via the latest estimate of damage functions and transition costs. Our linear setup, which captures first-order impacts, delivers closed-form results that we take to practical scenario analysis.

There are two broad types of physical climate risks. Chronic risks stem from gradual changes in global average surface temperature and precipitation patterns. Acute risks arise from extreme weather events and natural disasters, e.g., floods, hurricanes and wildfires. Empirical evidence shows that both types of physical risks can reduce global GDP and, therefore, consumption. In particular, persistently rising temperatures can curb long-term consumption growth via depressing productivity (Nath et al., 2024; Kotz et al., 2024). In the face of these damage threats, global warming mitigation policies contemplate the other side of the coin. Transition efforts to decarbonizing the world, however, also entail economic costs when curbing temperatures.

In consumption-based asset pricing, the stochastic discount factor (also known as the pricing kernel) is closely linked to consumption growth. Consequently, if rising temperatures or stricter temperature reduction policy targets reduce consumption growth, expected equity returns would inevitably be affected. This paper estimates how temperature-driven consumption damages translate into equity risk-premium and expected equity returns.

To study the impact of rising temperatures on expected equity returns, we extend a standard long-run risks (LRR) model to incorporate a persistent temperature state that affects consumption growth. The LRR model proposed by Bansal and Yaron (2004) has become one of the most influential frameworks in asset pricing and macrofinance. By introducing a small but persistent component of consumption growth, the model provides an explanation

for the equity premium puzzle, the risk-free rate puzzle, and the predictability of returns. Central to the framework are Epstein–Zin recursive preferences (Epstein and Zin (1989); Weil (1989)), which separate risk aversion from intertemporal substitution, allowing agents to assign disproportionate value to long-run risks. Since its introduction, the framework has been extended across asset classes and markets.

To incorporate the temperature-driven consumption damage, we introduce a dynamic temperature process which follows a policy target and allow consumption growth to be negatively impacted by a persistent component of temperature changes. The temperature dynamics are calibrated to the NGFS *Current Policies* scenario, under which the median temperature anomaly by 2100 is projected to reach about 3°C. Moreover, following (Nath et al., 2024; Kotz et al., 2024), we model the damages as persistent but not permanent reductions in the consumption growth. Concomitantly, to capture transition costs, we factor in the cost of implementing any given policy target. We calibrate the maximum range of potential transition costs on the basis of the NGFS *Net Zero 2050* scenario. Using a similar technique as in Bansal and Yaron (2004), Bansal et al. (2011), and Beeler and Campbell (2011), we derive closed-form expressions for the risk-free rate and the equity risk premium in this setting.

The first main finding is that the expected risk-free rate falls substantially during the rapid warming period and converges back to its long-run equilibrium level if the change of temperature fades. We take the standard LRR model as the counterfactual case, where the rising temperatures have no economic impact. In this counterfactual case, the expected risk-free rate is constant, representing the long-term general equilibrium rate. In contrast, with temperature-driven damages, the expected risk-free rate varies with the rising temperature. As the temperature rises and the damage to consumption growth intensifies, the expected risk-free rate falls. If the temperature stabilizes and the change of temperature fades, the expected risk-free rate gradually increases back to its long-run level. This behavior indicates that the stochastic discount factor is most affected during the period of rapid warming until

the economy progressively adapts to a new steady state.

A second main finding is that the temperature-driven damages and the transition costs raise the equity risk premium (ERP) also substantially. Despite a reduced ERP contribution of long-run risk because of the economic-to-temperature interplay, the temperature and policy states bring a net positive term on top of the premiums of the short-run and long-run consumption risks. In particular, if the temperature anomaly reaches 3°C by 2100, we find that the ERP is about 20% higher than the counterfactual case. Although the risk-free rate declines in both cases, the drop is smaller in magnitude than the increase in ERP. As a result, the expected equity return (i.e., the sum of the risk-free rate and the ERP) in both cases becomes higher than the counterfactual level, implying potential losses of asset values in a warming environment.

Our extended LRR framework is flexible enough to study different channels through which the rising temperature can affect risk premiums. In particular, we allow the volatility to increase with temperature, meaning that global warming would also bring more economic uncertainty while temperatures climb. Our third main finding is that, with stochastic volatility linked to temperature, equity risk premium becomes state, or more precisely temperature-change, -dependent.

Our work is related to the asset pricing literature on climate risks and equity markets. The closest studies are Bansal et al. (2016, 2019), which also extend the standard LRR model to include a temperature risk. In their setting, the climate risk is introduced via a jump process that represents arrivals of natural disasters. Therefore, their models intend to study the impact of tipping points on the financial market, and they lack reasonable calibration. In contrast, we focus on the chronic climate risks, and we manage a precise model calibration. By incorporating a persistent component of the change of temperature, our model allows calibrations to a broad set of econometric estimates from the empirical literature. Our analytical and numerical results support the findings in Bansal et al. (2016, 2019), namely, the equity risk premium will increase due to the impact of physical climate

risk. Eventually, a key additional contribution of our work is to not only study physical damages, but also transition costs.

Other related works include Barnett et al. (2020) and Giglio et al. (2021), which also apply the LRR model to examine uncertainty about climate change damages and long-run productivity, highlighting the role of persistent risks in environmental economics. These climate finance models highlight welfare and policy trade-offs in the presence of long-run economic uncertainty. Yet, they either focus on the theoretical interplay of multiple layers of uncertainties or concentrate on climate-sensitive markets. We, on the other hand, streamline the key channels of climatic influences, calibrate them to refine the expected magnitude of risk premia and conclude that climate risks are significant for the broad financial market.

Meanwhile indeed, a rapidly expanding empirical literature examines how physical climate risks are priced in financial markets. Giglio et al. (2021) provide foundational evidence that long-horizon sea-level-rise risk is capitalized into U.S. municipal bond prices, a result reinforced by the housing-market findings of Bernstein et al. (2019) and Baldauf et al. (2020), who show that coastal property values reflect rising flood risk. Complementary work by Painter (2020) documents higher municipal bond yields in counties more exposed to sea-level rise, while Addoum et al. (2023) link abnormal local weather to cross-sectional equity returns. At the global equity level, Engle et al. (2020) construct a tradable *climate news hedge portfolio* that earns positive returns when unexpected climate-related information hits markets, demonstrating that investors can hedge climate-news shocks directly. Pástor et al. (2021) show that "green" stocks command lower expected returns when climate concerns strengthen, consistent with investor-hedging motives. Echoing these theoretical prediction, Bua et al. (2024) reports that in European markets heightened physical risk lowers returns on "green" assets relative to "brown" ones. Cross-country evidence from Zhang (2022) indicates that equity markets in emerging economies react less to news about physical climate risks than developed markets despite greater underlying vulnerability. Factor-model approaches such as Gostlow (2024) construct granular physical-risk factors—hurricanes, heat stress,

sea-level rise, and extreme rainfall—and find positive premia for hurricane risk but weak pricing of the other components. Additional highly cited contributions include Hong et al. (2021), who document that U.S. equity markets price drought and temperature anomalies. Together, these studies show that investors increasingly demand compensation for both acute and chronic climate hazards across real estate, fixed income, and global equity markets. We provide quantified estimates of how high these exact numbers could go.

In a nutshell, as temperature continues to rise, the economy enters an unknown future. Because historical data provide limited guidance for such nonstationary environments, it is hard to quantify the financial impact of climate risk by backwards-looking data-driven approaches. Structured asset-pricing frameworks that incorporate the mechanisms of climate damages and potential efforts to limit them are therefore essential for forward-looking analysis. Our contribution is a tractable extension of a stylized macro–asset-pricing model with an explicit climate channel. The temperature state is calibrated to benchmark climate scenarios and embed warming sensitivity to economic activity, while empirical econometric estimates of transition costs and physical damage functions are incorporated. In this sense, the model offers a useful platform for theoretical and empirical analysis of how climate risk transmits to equity markets.

The rest of the paper is organized as follows. Section 2 provides the modeling framework, i.e., the modular asset pricing model with climate module interacting with the long-run risk economic module. It also details the calibration procedure for all the components. In section 3, closed-form expressions of the model solutions are presented, including risk-free rate, price-dividend ratios and the various risk premia. Section 4 provides quantitative temporal profiles of the asset-pricing variables of interest together with a range of sensitivity investigations. The last section concludes and discusses potential future research directions. All technical proofs and supporting material are located in the appendix.

2 Model setup and calibration

This section introduces our framework, which integrates a reduced-form climate model into a consumption asset-pricing workhorse. We present the calibration strategies for each module, and the full set of parameters identified by our detailed calibration is listed in Table 6 of Appendix D.

2.1 Temperature dynamics with persistent climate policy

Climate physics is complex, yet well understood, with all its uncertainties. We aim to capture the basic salient features of global warming likely trajectories, tied to policy decisions. Let T_t be the temperature anomaly at time t and P_t be a numeric metric of the transition policy state. The temperature dynamics are given by

$$T_{t+1} = \nu T_t + (1-\nu)P_t + \Theta x_t + \sigma_\zeta \zeta_{t+1}, \tag{1}$$

$$P_{t+1} = \alpha P_t + (1-\alpha)\bar{P} + \sigma_\iota \iota_{t+1}, \tag{2}$$

$$\zeta_{t+1}, \iota_{t+1} \sim \mathcal{N}(0,1).$$

The temperature state is modeled by a double-mean reverting process. The stochastic temperature state T_t converges to the latent policy process P_t, while the policy process itself converges to the long-term temperature target $\bar{P}$. The parameter $0 < \alpha < 1$ denotes the persistence of the policy. The policy state P_t can be understood as the policy-driven temperature target. For instance, if $\bar{P} = 0°\text{C}$, the expected temperature will converge back to the pre-industrial level. The additional term Θx_t captures the impact of economic activity's overheating or underheating compared to a reference trajectory, and its impact on physical temperatures. In expectation, this term is zero, and we discuss its meaning and calibration precisely in sections 2.3 and 2.3.3.

Note that the temperature dynamics in equation (1) are not mechanical representations

of temperature anomalies as described by the two-layer or three-layer models (Geoffroy et al., 2013a,b; Tsutsui and Smith, 2024; Leach et al., 2021). On the one hand, a rigorous interaction of temperatures and transition policies will involve more states, which makes the model significantly more complicated. On the other hand, deep uncertainty exists in the mechanism of rising temperatures. The impact of those uncertainties in climate science is out of the scope of the current study. Therefore, we introduce a simple but tractable temperature model that can be easily calibrated to represent the temperature projections under recent benchmark climate scenarios such as those developed by IPCC and NGFS. Climate model uncertainty is captured in a parsimonious manner by the temperature process volatility.

Climate policy targets vary in time and are not determined by physical determinism. Yet, a key feature of these targets that is supported by empirical experience is that they are slow-moving phenomena that may revert over time. We capture these salient features and accompanying uncertainties.

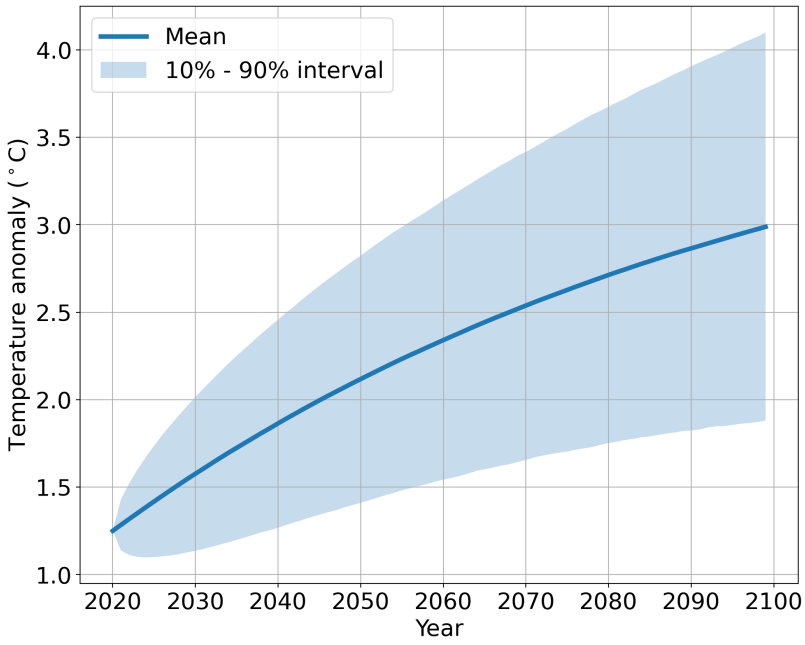

Figure 1: **Distribution of temperature trajectories.** The distribution of temperatures in 2100 has the following quantiles: Q10 = 1.9, Q50 = 3.0, Q90 = 4.1.

Calibration. As far as calibration is concerned, the parameters ν, α and $\bar{P}$ are determined so that the mean trajectory of our temperature process mimics the path of temperatures envisioned by scenarios where current climatic efforts are neither increased nor decreased. We use as a benchmark the NGFS (2024b) current policy scenario, and Figure 7 in Appendix E.1 presents the fitting. Together, the three parameters command the level, slope and curvature of the trajectory.

The parameter σ_ι measures policy uncertainty and σ_ζ measures uncertainty in temperature models. We use published temperature projections across different climate policy scenarios, such as NGFS and IPCC to quantify σ_ι. In the absence of model uncertainty (i.e., $\sigma_\zeta = 0$), we calibrate σ_ι such that simulated temperature paths cover all projections under the NGFS scenarios and map scenarios to conditional quantiles. In particular, the 95th percentile of 2100 temperature is below 4.1 °C, corresponding to the projection by the SSP2-Baseline scenario. Figure 8 in Appendix E.1 presents the fitting. Then, within any given policy scenario, NGFS provides different percentiles of temperature projections that reflect model uncertainty. We calibrate the parameter σ_ζ such that, under the "Current Policies" scenario, the simulated temperature paths cover the reported percentile range of temperature projections by NGFS. Figure 9 in Appendix E.1 presents the fitting.

Figure 1 presents the distribution of trajectories generated by our calibrated climate module.

2.2 Lasting but not permanent impact of rising temperatures

A lingering discussion in the climate-economics literature has been to envision whether global warming would have permanent or transitory impacts. The latest empirical studies (see Appendix A) points towards a middle ground. To model temperatures that have a lasting but not permanent impact, we define a persistent component of changes in temperatures as

follows:

$$Y_{t+1} = \beta Y_t + T_{t+1} - T_t + \sigma_\omega \omega_{t+1}, \tag{3}$$
$$Y(0) = 0, \quad \omega_{t+1} \sim \mathcal{N}(0,1).$$

The process Y_t is a function of changes of temperatures and is persistent with the parameter $0 < \beta < 1$. The standard normal random variable ω_t is independent of other shocks and denotes the characteristic uncertainty in the Y_t process.

Calibration A higher value of β means that one shock of the temperature will have a longer impact on the system, and vice versa. According to Kotz et al. (2024), the persistence of the temperature impact can be as long as 10 years. Therefore, we calibrate β such that the impact of one unit of temperature change after 10 years is below 1% (see Figure 10 in the Appendix for an illustration).

The parameter σ_ω measures the uncertainty of this temperature change signal. Since the true window of temporal impact of climate change is uncertain, we calibrate the σ_ω so that the highest and lowest deciles of the process distribution capture an equivalent memory range of 5 to 15 years. Figure 11 in Appendix E.1 presents the fitting.

2.3 The long-run risks model with climate extension

We incorporate our climate module into the long-run-risks asset pricing workhorse. The standard LRR model (Bansal and Yaron, 2004) without the impacts of climate change represents the counterfactual world. Let Δc_{t+1} denote the consumption growth between t and $t+1$. Let x_t be the latent long-run-risk process. Here, $\mu > 0$ is the equilibrium consumption growth. The persistence parameter $0 < \rho < 1$ is the key to the long-run risk process. A shock of the long-run risk will have a longer-lasting impact with a higher value of ρ. Integrating

the temperature dynamics with the market dynamics, our model is then given by

$$\Delta c_{t+1} = \mu + x_t + \Omega Y_{t+1} + \Gamma(P_{t+1} - \bar{P}) + \sigma_{\eta,t}\eta_{t+1}, \tag{4}$$

$$x_{t+1} = \rho x_t + \sigma_{\epsilon,t}\epsilon_{t+1}, \tag{5}$$

$$\eta_{t+1}, \epsilon_{t+1} \sim \mathcal{N}(0,1).$$

The components ΩY_{t+1} and $\Gamma(P_{t+1} - \bar{P})$ in equation (4) are overlayed to respectively capture physical and transition risks. $\Omega < 0$ is the damage parameter of the persistently rising temperatures on the consumption growth. $\Gamma > 0$ is the transition cost parameter linking deviations from the baseline policy to impacts on the economy. In the counterfactual scenario, we have $\Omega = 0$ and $\Gamma = 0$. Eventually, the economic feedback to temperature Θx_t, with $\Theta > 0$, is already incorporated in equation (1) to capture the feeding loop of long-term economic activity deviating from trend to physical temperature.

2.3.1 Damages

Physical risks usually mean the risks from the gradual change of global average surface temperature (i.e., temperature anomaly), precipitation patterns and other acute events (e.g., flooding, droughts, wildfire). All of these phenomena are highly correlated to atmospheric temperature, and the literature estimating damages highlights that temperature is the main explanatory variable of economic impact.

Calibration. The calibration of the channel through which climate damages the consumption growth follows the most recent econometric estimates. Table 5 presented in Appendix A summarizes projected losses, measured relative to a counterfactual GDP trajectory, at 2 °C and 3 °C above pre-industrial levels across a selection of studies. Conservative early estimates suggest losses of about 2% of global GDP, while high-end, more recent estimates reach 44% by 2100. Early damage function estimates underestimated potential downside

risks of climate change (DeFries et al., 2019). More recent estimates, either from top-down incorporation of non-diversifiable temperature exposures (Bilal and Känzig, 2024), or from bottom-up capture of local dynamics (Burke et al., 2015; Kotz et al., 2024), have converged on substantial potential losses.

	Low Damage (Kotz et al. (2024))	High Damage (Bilal and Känzig (2024))
Damage parameter Ω	-0.0102	-0.0146
Expected Damage level at 3°C	-33%	-44%
Persistence of temperature change	10 years	10 years

Table 1: **Calibration of damage parameter to empirical literature estimates.** The calibrated "Low Damage", our benchmark, and "High Damage" scenarios.

We calibrated two damage scenarios based on the recent empirical estimates (Table 1), making the assumption that GDP damages are passed through to consumption. In both scenarios, the expected temperature rises to about 3°C by 2100, consistent with the projections by the NGFS Current Policy scenario. The two scenarios differ in the expected consumption loss by 2100. Under the "Low Damage" scenario, the expected consumption loss by 2100 is about 33% compared with the counterfactual level, following the estimate in Kotz et al. (2024). This loss corresponds to $\Omega = -0.0102$. Under the "High Damage" scenario, the consumption loss associated with a 3°C temperature anomaly rises to 44% according to the estimate in Bilal and Känzig (2024). In this case, we calibrate that $\Omega = -0.0146$. In both scenarios, the impact of rising temperatures is assumed to last for as long as 10 years. This indicates a persistent but not permanent impact of the temperature change. Figure 12 in Appendix E.3 illustrates the expected consumption under the two damage scenarios in comparison with the counterfactual consumption. To ensure that our risk estimates remain conservative, we use the "Low Damage" calibration as our benchmark.

2.3.2 Transition costs

Achieving climate objectives that depart from the outstanding laissez-faire dynamics entails economic costs –or bonuses. In our setting, P_t captures the climate target, so adding to the consumption growth process a transition cost term $\Gamma(P_{t+1} - \bar{P})$, with $\Gamma > 0$, leads to an economic drag when temperature targets are lowered, and a boost when targets are allowed to drift higher.

Calibration. The Γ parameter is calibrated to capture the potential impact of transition costs on the economy. We anchor our calibration to the transition costs estimates produced by NGFS (scenario profiles are in Figure 13 of Appendix E.4). Namely, we map the cost of the most progressive transition scenario proposed by NGFS, "Net Zero 2050", to the consumption reduction that the lowest quantile of our temperature distribution would trigger. The calibration process is then similar to that of the damages explained just before.

2.3.3 Economic impact on temperatures

While the central trajectories of our physical system in equations (1) and (2) mirror the current policies of an SSP2 economic environment, stronger (or weaker) activity would impact temperatures. The long-term consumption growth variable x_t exactly captures such a departure from the central trajectory, and the Θx_t term, with $\Theta > 0$, in equation (1) embeds the fueling effect. The Θ parameter is calibrated to capture the range of temperature trajectories that may be fuelled by a wide range of economic trajectories envisioned by the IPCC.

Calibration. We start by acknowledging that the realm of Shared Socioeconomic Pathways (SSPs) envisioned by the IPCC presents average global economic growth rates within 1% annual growth rate from the medium SSP2 scenario (see Table 7 in Appendix E.5). Namely, GDP growth in SSP5 (respectively SSP3) is 1 percentage point higher (respectively

lower) than that of SSP2. Then, as presented in Figure 14 we calibrate the impact parameter Θ so that the range of temperatures achieved purely by a 1 percentage point permanent increase of activity growth leads to a temperature of 5°C by the end of the century, typically considered in the climate literature as a temperature level that would start jeopardizing human life on Earth, in the last percentile of the temperature distribution.

2.4 Stochastic volatility linked to temperature

We have modeled so far the damage channel through which global warming would hurt economic growth. Yet, rising temperatures are likely also to increase variability (Addoum et al., 2020) and uncertainty (Barnett et al., 2020) within the climate-economic system. We account for this additional risk by allowing for temperature-dependent. stochastic volatilities. More precisely, we assume that volatility of the processes may scale linearly with the Y_t process

$$\sigma_{j,t} = \sigma_j \sqrt{1 + \pi_j Y_t} \quad \forall j \in \{\eta, \epsilon\}, \tag{6}$$

such that this effect is only transient[1] until climate patterns equilibrate.

Note that the standard LRR model can include a mean-reverting stochastic volatility process (Bansal and Yaron, 2004), which adds to financial market uncertainty and shares the equity-risk-premium contribution. We keep to the first version of the LRR model to keep the original long-run contribution to a single channel. However, including an autoregressive pattern in our stochastic volatilities would not change our conclusions.

Calibration. While historical data provides limited guidance to evaluate the π coefficients, we are in a position to run sensitivity analysis under different scenarios. We calibrate the π coefficients so that on the central path of the Y_t process, volatility is increased by a maximum of 10%. In our reference calibration, we only consider stochastic volatility on the short-run consumption process $\pi_\eta > 0$, but not the long-run one, $\pi_\epsilon = 0$. Numerical sensitivity analysis in section 4.2 relaxes this assumption and shows that our assumption errs on the conservative side.

[1] In an alternate version of the model where volatility increases with temperature levels instead, the impacts are permanent.

3 Closed-form solutions

Analytical expressions for the stochastic discount factor, risk-free rate and the equity risk premium are presented.

3.1 The prices of risks

We assume that the representative agent has an Epstein-Zin-type recursive preference (Epstein and Zin, 1989; Weil, 1989). Let γ be the relative risk aversion; ψ be the elasticity of intertemporal substitution. As shown by Bansal et al. (2005) and Beeler and Campbell (2011), the logarithm of the stochastic discount factor M_{t+1} is given by

$$m_{t+1} := \ln M_{t+1} = \theta \ln \delta - \frac{\theta}{\psi}\Delta c_{t+1} + (\theta - 1) r^c_{t+1}, \quad \theta = \frac{1-\gamma}{1-1/\psi}. \tag{7}$$

Here, the parameter $\delta > 0$ measures the subjective discount factor of future utilities. Moreover, $r^c_{t+1} := \ln \frac{W_{t+1}}{W_t - C_t}$ represents the return on the aggregate wealth portfolio that generates consumption flows, in which W_t denotes the price of the aggregate wealth portfolio (or equivalently the present value of future consumptions). Let $z^c_t := \ln(W_t/C_t)$ denote the log of the price-consumption ratio. The return r^c_{t+1} can be rewritten as

$$r^c_{t+1} = z^c_{t+1} + \Delta c_t - \ln(\exp(z^c_t) - 1).$$

We can see that the stochastic discount factor (7) is closely related to the consumption growth and the value of future consumptions. The price of the aggregate wealth portfolio equals the present value of future consumptions. Therefore, z^c_t indicates the relative price of future consumptions and today's consumptions. Let $\bar{z}^c$ denote its equilibrium value. When $z^c_t > \bar{z}^c$, the agent perceives a higher value of future consumption, which suggests an optimistic view of the future or a booming market. On the contrary, when $z^c_t < \bar{z}^c$, the agent perceives less value of future consumptions, implying a worse market state. Thus, the log-price-consumption

ratio z_t^c endogenously reflects the change of the stochastic discount factor.

As is standard in LRR models, we posit and verify that the log-price-consumption ratio z_t^c is linearly dependent (i.e., an affine function) of the state variables.

$$z_t^c = A_0^c + A_1^c x_t + A_2^c T_t + A_3^c Y_t + A_4^c P_t.$$

In Appendix B.1 we detail how we identify the constant $A_c's$ from the Euler equation.

From the specification of our framework detailed in section 2, our model includes five mutually independent risks,

1. the short-run consumption risk η_t,
2. the long-run consumption risk ϵ_t,
3. the temperature level risk ζ_t,
4. the temperature change risk w_t,
5. the policy risk: ι_t.

We use λ_η, λ_ϵ, λ_ζ, λ_ω and λ_ι to denote the price of these risks, respectively. The price of risk measures the sensitivity of the stochastic discount factor to a particular risk. The innovation of the stochastic discount factor can be written as

$$m_{t+1} - \mathbb{E}[m_{t+1}|m_t] = -\sum_{j\in\{\eta,\epsilon,\zeta,\iota,\omega\}} \lambda_j \sigma_j j_{t+1}. \tag{8}$$

Lemma 1 gives the analytical expressions of the price of each risk. The proof is detailed in Appendix B.1. We denote by β_η^c, β_ϵ^c, β_ζ^c, β_ι^c and β_w^c the corresponding exposures of the aggregate wealth portfolio to these risks.

Lemma 1. *Let define* $\kappa_1^c := \frac{e^{\bar{z}^c}}{e^{\bar{z}^c}-1}$ *and* $\kappa_0^c := \kappa_1^c \bar{z}^c - \ln(e^{\bar{z}^c} - 1)$*, where* $\bar{z}^c$ *is the long term equilibrium value of the log-price-consumption ratio. The closed-form formulas for the five risk prices are listed in Table 2.*

Risk	Parameter	Formula
short-run consumptionn	λ_η	γ
long-term consumption	λ_ϵ	$(1-\theta)A_1^c$
temperature change	λ_ω	$(1-\theta)A_3^c + \gamma\Omega$
temperature level	λ_ς	$(1-\theta)(A_2^c + A_3^c) + \gamma\Omega$
policy	λ_ι	$(1-\theta)A_4^c + \gamma\Gamma$

Table 2: **Risk prices.** Closed-form formulas.

The signing proof in Appendix C highlights that the prices of the short-run and the long-run consumption risks are positive. From Eq. (8), we see that a positive shock to these risks will lead to a smaller stochastic discount factor m_{t+1}, and hence a higher risk-free rate, which is consistent with periods of stronger expected consumption growth. However, the prices of temperature change and temperature level risk, are in most cases negative. Therefore, positive shocks to these risks raise the stochastic discount factor, decreasing the risk-free rate, which is consistent with weaker expected consumption growth due to damage costs. Policy risk in the end is facing a tug of war, and its sign depends on the relative strength of physical versus transition costs. Transition costs may be endured so that damages are avoided, leaving a net-beneficial effect. In our preferred calibration policy risk contributes positively to the risk-free rate.

3.2 The risk-free rate

The risk-free rate between t and $t+1$ is defined as

$$r_{f,t} = -\mathbb{E}[\exp(m_{t+1})|m_t]. \tag{9}$$

Proposition 1 provides the risk-free rate as a state-dependent process, and its proof is provided in Appendix B.2.

Proposition 1. *The risk-free rate $r_{f,t}$ is given by*

$$r_{f,t} = r_f + \frac{1+\Omega\Theta}{\psi}x_t + \frac{\Omega\beta}{\psi}Y_t + (1-\nu)\frac{\Omega}{\psi}[P_t - T_t] + \alpha\frac{\Gamma}{\psi}[P_t - \bar{P}] + \left[\left(1-\frac{1}{\theta}\right)\frac{V_2^{ec}}{2} - \frac{V_2^e}{2}\right]Y_t \tag{10}$$

$$r_f = -\log\delta + \frac{1}{\psi}\mu + \left(1-\frac{1}{\theta}\right)\frac{V_1^{ec}}{2} - \frac{V_1^e}{2} \tag{11}$$

with the constant terms

$$V_1^e = \sum_{j\in\{\eta,\epsilon,\zeta,\iota,\omega\}} \lambda_j^2\sigma_j^2 \tag{12}$$

$$V_2^e = \sum_{j\in\{\eta,\epsilon,\zeta,\iota,\omega\}} \pi_j\lambda_j^2\sigma_j^2 \tag{13}$$

$$V_1^{ec} = \sum_{j\in\{\eta,\epsilon,\zeta,\iota,\omega\}} (\beta_j^c - \lambda_j)^2\sigma_j^2 \tag{14}$$

$$V_2^{ec} = \sum_{j\in\{\eta,\epsilon,\zeta,\iota,\omega\}} \pi_j(\beta_j^c - \lambda_j)^2\sigma_j^2 \tag{15}$$

so that the expected risk-free rate converges to the constant rate r_f

$$\lim_{t\to\infty}\mathbb{E}[r_{f,t}] = r_f.$$

In our model, the risk-free rate consists of a constant term r_f and temperature-adjusted state-dependent terms. The damage term ΩY_t reduces the risk-free rate until temperatures stop increasing. The transition costs $\Gamma(P_t - \bar{P})$ also reduce the risk-free rate on low temperature policy paths. Before the temperature converges to the policy target level, the expected risk-free rate is impacted by the gaps $(P_t - T_t)$ in the climate system. The last term stems from the stochastic volatility process and evolves with its state-variable Y_t.

As the temperature converges and the gap to policy fades, the climate impact phases out, and the risk-free rate converges to the long-term equilibrium level r_f. It is the sum of the standard time-discount rate and of the consumption growth rate drift scales by the elasticity

of intertemporal substitution, augmented by the Epstein-Zin volatility adjustment factor.

In the counterfactual case, the risk-free rate only depends on the single long-run risk state x_t. In particular, the expected risk-free rate is a constant as $\mathbb{E}[x_t] = 0$. Adding climate impacts, the risk-free rate depends not only on the market's long-run risk state but also on the climate processes.

3.3 The equity risk premia

The market-representative equity portfolio is a leveraged wealth portfolio and pays a dividend stream d_t where $\varphi > 1$ captures dividend leverage relative to consumption, typically $\varphi \in (1, 3)$.

$$\begin{aligned} \Delta d_{t+1} &= \varphi \Delta c_{t+1} + (1-\varphi)\left[\mu + \Omega \hat{Y}_{t+1}\right] + \sigma_{u,t} u_{t+1}, \\ u_{t+1} &\sim \mathcal{N}(0,1), \end{aligned} \tag{16}$$

where the deterministic processes $\hat{T}$ and $\hat{Y}$ are the alter-ego of the T and Y processes,

$$\hat{T}_{t+1} = \nu \hat{T}_t + (1-\nu)\bar{P}, \tag{17}$$

$$\hat{Y}_{t+1} = \beta \hat{Y}_t + \hat{T}_{t+1} - \hat{T}_t. \tag{18}$$

The second term in Equation 16 ensures that dividends grow a the same pace as aggregate consumption.

Let r^d_{t+1} be the equity portfolio's return between t and $t+1$. The Euler equation ensures that

$$\mathbb{E}[\exp(m_{t+1} + r^d_{t+1})] = 1. \tag{19}$$

and the standard guess-and-verify process hinges on a price-dividend ratio linear in the state variables

$$z^d_t = A^d_0 + A^d_1 x_t + A^d_2 T_t + A^d_3 Y_t + A^d_4 P_t + A^d_5 \hat{T}_t + A^d_6 \hat{Y}_t.$$

The derivations of the closed-form formulas to compute A^d's are provided in Appendix B.3.

Let $\beta_j^d, j \in \{\eta, \epsilon, \zeta, \iota, \omega\}$ denote the exposures of the equity portfolio to the five risks in our model.

Lemma 2. *Let* $\kappa_1^d = \frac{e^{\bar{z}^d}}{\exp(\bar{z}^d)+1}$ *and* $\kappa_0^d = \ln(e^{\bar{z}^d}+1) - \kappa_1^d \bar{z}^d$, *where* $\bar{z}^d$ *is the long term equilibrium value of the log-price-dividend ratio. The closed-form formulas for the risk exposures of the dividend process are listed in Table 3.*

Risk	Parameter	Formula
short-run consumptionn	β_η^d	φ
long-term consumption	β_ϵ^d	$\kappa_1^d A_1^d$
temperature change	β_ω^d	$\kappa_1^d A_3^d + \varphi\Omega$
temperature level	β_ζ^d	$\kappa_1^d (A_2^d + A_3^d) + \varphi\Omega$
policy	β_ι^d	$\kappa_1^d A_4^d + \varphi\Gamma$

Table 3: **Dividends' risk exposures.** Closed-form formulas.

The exposures to the short-run and the long-run consumption risks are positive. This is because a positive shock of these risks will increase consumption growth. Consequently, dividend growth also increases as it is positively correlated to consumption growth. On the contrary, as is detailed in Appendix C the exposures of the temperature-related risks are negative, because positive shocks of these risks will damage consumption growth. On the policy front, the tug of war is still at play, yet the larger the leverage ϕ, the more likely the exposure β_ι^d turns positive.

The equity risk premium, i.e., the excess return of the equity portfolio,

$$ERP_t^d := \ln\left(\mathbb{E}[\exp(r_{t+1}^d - r_{f,t})]\right) = \mathbb{E}[r_{t+1}^d - r_{f,t}] + \frac{1}{2}Var(r_{t+1}^d) = -Cov(m_{t+1}, r_{t+1}^d),$$

can be expressed in analytical form in our setup.

Proposition 2. *The equity risk premium,* ERP_t^d, *can be expressed as*

$$ERP_t^d = \sum_{j\in\{\eta,\epsilon,\zeta,\iota,\omega\}} \beta_j^d \lambda_j \sigma_j^2 + \sum_{j\in\{\eta,\epsilon\}} \pi_j \beta_j^d \lambda_j \sigma_j^2 \quad Y_t. \tag{20}$$

The equity risk premium is temperature-dependent when at least one of the processes of the model carries temperature-dependent volatility.

Recall from the discussion following Lemma 1 and Lemma 2 that the prices of risks and the exposures are in most cases of the same sign, with the only caveat on policy risk. As a result, the ERP incorporating the climate damage will be larger than the counterfactual. Policy risk typically also contributes to it, except in some cases when risk aversion γ is small.

4 Quantitative results

4.1 Benchmark calibration and temporal profiles

The time-profiles of the financial variables recovered by our framework highlight meaningful patterns.

First, the real risk-free rate of our model sags c. 50bps compared to counterfactual, i.e. 20% of its value, at the peak of the global warming pass-through in the decade around 2040. It remains lower than counterfactual by the end of the century by c. 25bps. As can be visualized in Figure 2, under the more acute "high damage" scenario, the risk-free rate through is c. 1pp lower than counterfactual. The risk-free rate pathways are inversely sensitive to increasing transition Γ and display no sensitivity to Θ (cf. Figures 15 and 16 in the Appendix).

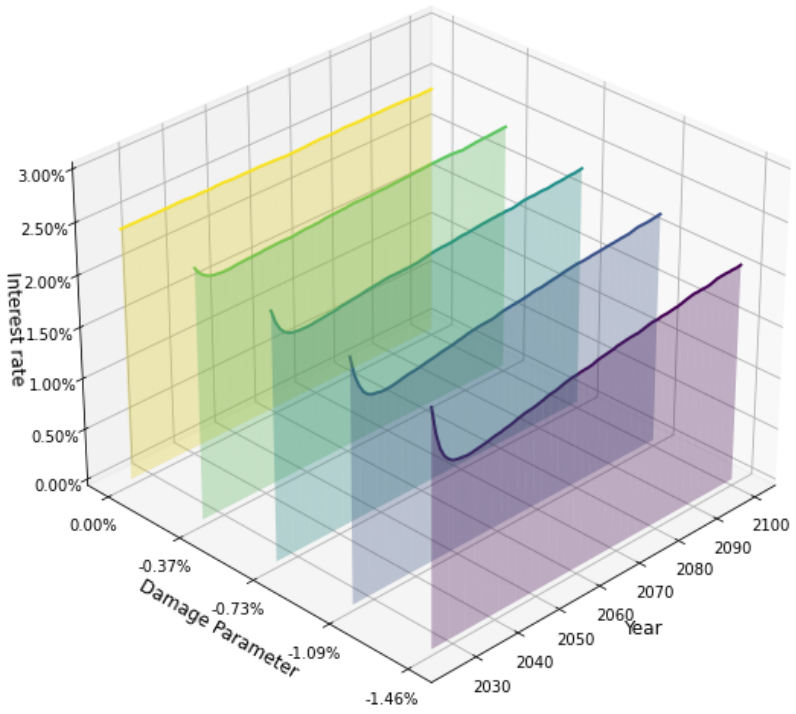

Figure 2: **Risk-free rate time-profile for different damages.** Time-profile of the risk-free rate $r_{f,t}$ on the mean trajectory of the state-variables when the damage parameter decreases from counterfactual (0%) to high damage (-1.46%) calibration. $\Gamma = 0.00045, \Theta = 0.2, \pi_\eta = 0$

Second, the equity-risk premium is also time-dependent as visible in Figure 3, but only from the short-run consumption contribution. More striking is the increase in ERP from climate risks, and their contribution to the total despite a haircut on long-run risk.

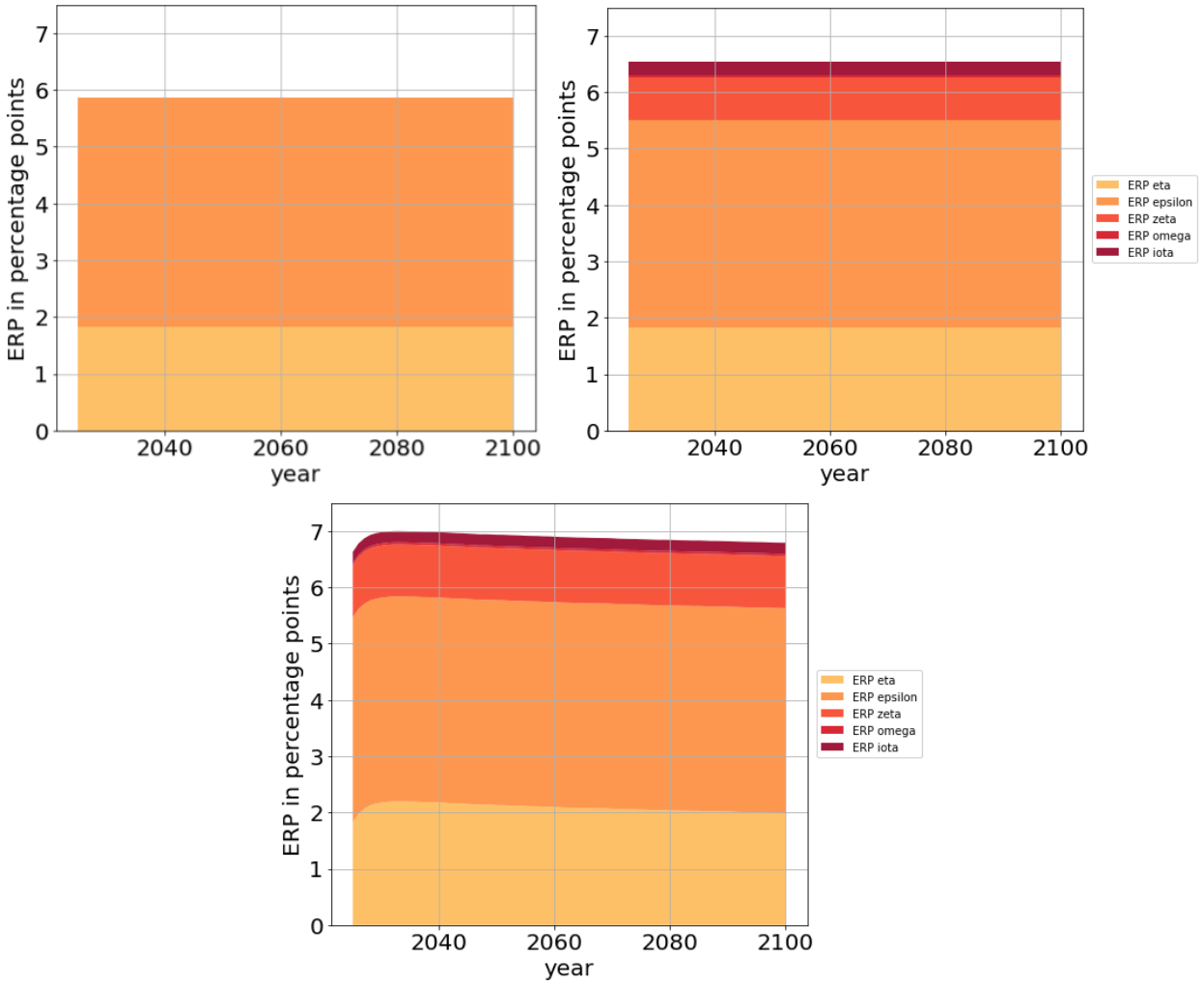

Figure 3: **Equity Risk Premium composition time-profile.** Time-profile of the equity risk premia on the mean trajectory of the state-variables at reference calibration for three setups: counterfactual in the top LHS chart, with climate but no stochastic volatility in the top RHS chart, and with climate also impacting volatility in the bottom chart.

Table 4 presents the contribution of each risk (in percentage) to the total ERP. In the counterfactual case, c. 30% of the ERP comes from the short-run risk and c. 70% is from the long-run risk. As we introduce climate risk[2], the additional ERP (damage, transition,

[2]Figure 17 in Appendix F details the level comparison to counterfactual for all five components.

temperature and policy risk) accounts for c. 13.4% of total ERP which is of the same scale than the contribution of the short-run consumption risk.

	Short-Run consumption	Long-Run consumption	Temperature level	Temperature change	Policy target
Counterfactual	31.1%	68.9%	0	0	0
Climate calibration	27.9%	56.3%	11.6%	0.6%	3.6%

Table 4: **Contributions of each type of risk to equilibrium ERP.**

Third, the price dividend ratio is typically reduced by c. 4% in our benchmark calibration.

4.2 Sensitivity analysis

Sensitivity analysis in Figure 4 highlights that increasing damage costs via higher Ω contributes primarily to the risk premia contribution of temperature level risks, and to a lesser extent to temperature change risk, while it reduces the policy risk contribution stemming from transition risks. Indeed, conversely to damage, increasing transition costs Γ impacts policy risks in a non-monotonic manner, first counteracting the damage channel, before adding policy risk. Both shave off some contribution from the long-run consumption risk. This latter structural contribution to risk is further dented by the impact, from higher Θ, of economic activity on physical temperature.

Figure 4 also details the impact of stochastic volatility on the five risk contributors. π_ϵ has a substantially stronger impact than π_η.

Eventually, Figure 5 and 6 underline the impact of both physical and transition costs on price-dividend and price-consumption ratios[3]. The former is relatively more sensitive to damage risk, while the latter is predominantly sensitive to transition risks.

[3]The sensitivity analysis always considers the calibrated Θ channel, yet we highlight that when $\Omega = \Theta = 0$ the climate module has no impact on the economic module, which corresponds to the counterfactual case as far as asset pricing is concerned.

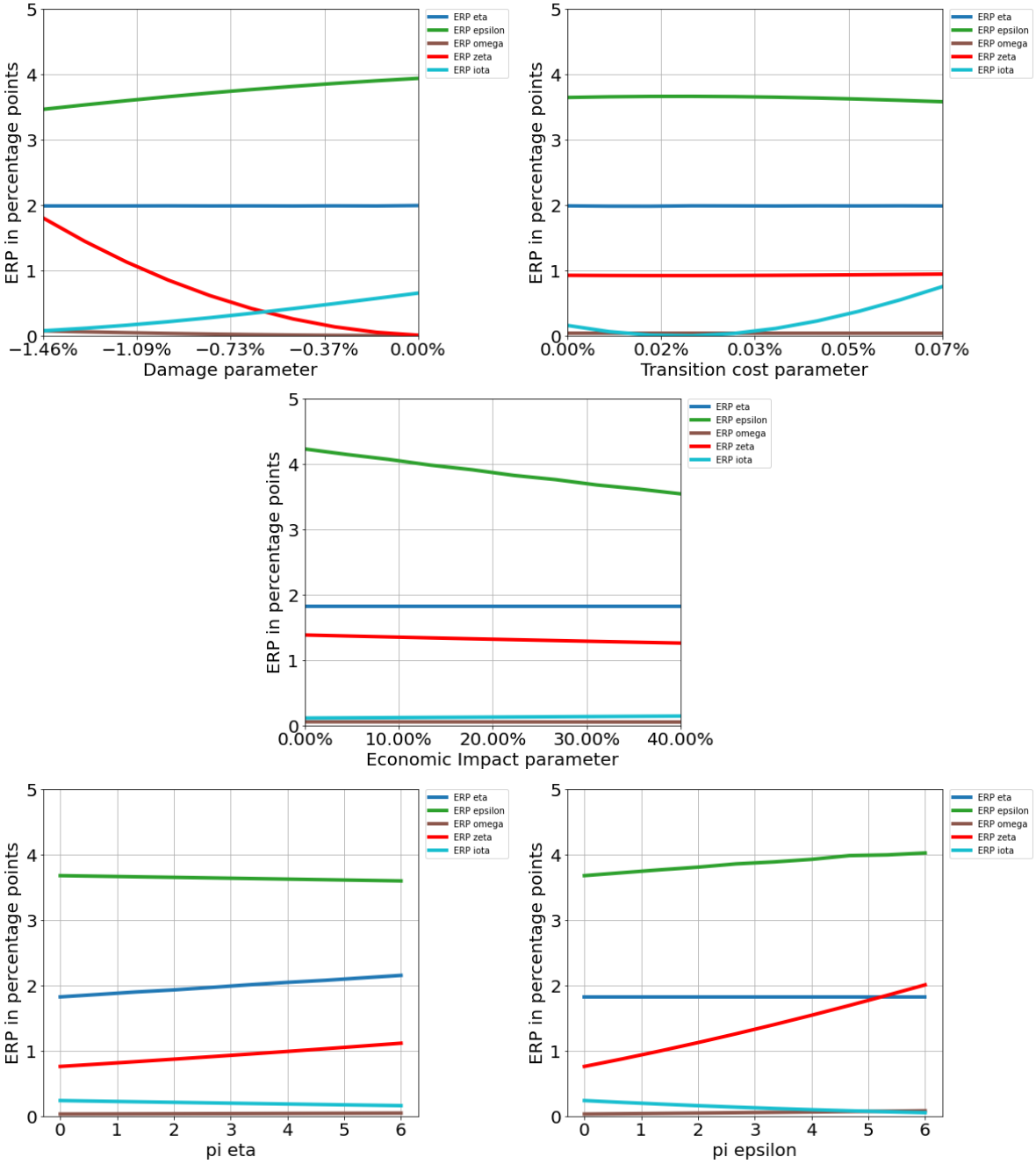

Figure 4: **Sensitivity analysis of Equity Risk Premia to climate-related parameters.** Five expected risk premia at horizon 2100, as five key climate parameters of the model, Ω, Γ, Θ, π_η and π_ϵ, vary independently from the default calibration.

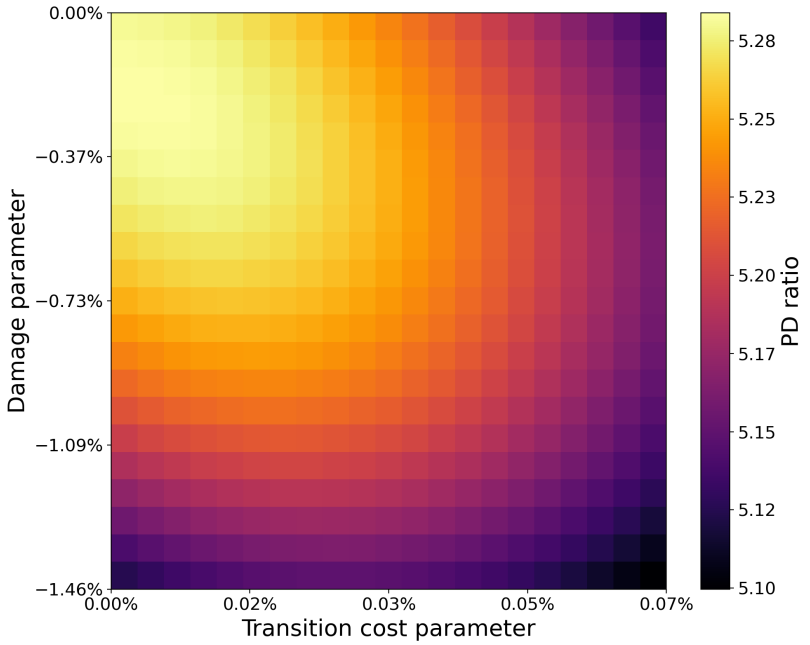

Figure 5: Response of the (equilibrium log) price-dividend ratio to varying transition costs and consumption damages.

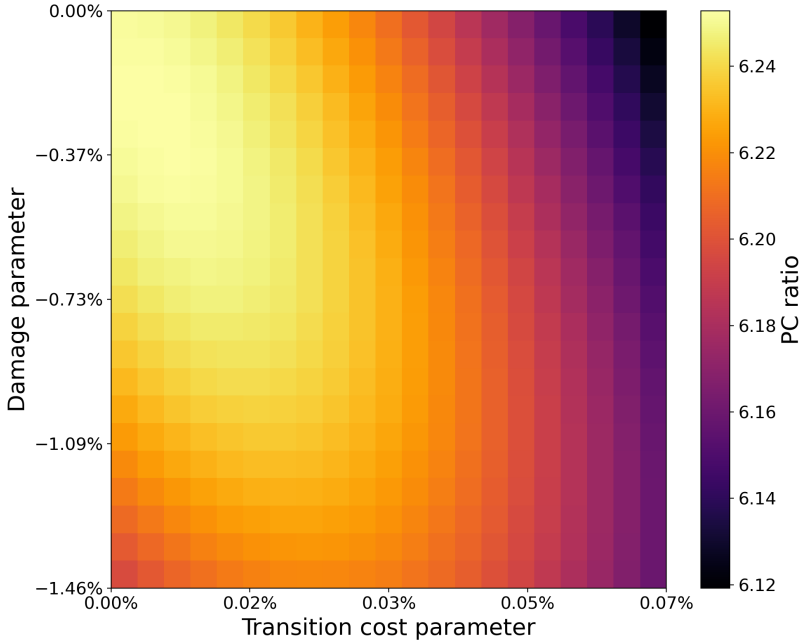

Figure 6: Response of the (equilibrium log) price-consumption ratio to varying transition costs and consumption damages.

5 Concluding remarks

This paper develops a tractable, forward-looking framework to quantify how physical and transition climate risk affects asset pricing. By embedding a persistent temperature process into a standard long-run risks model, we show analytically and numerically that rising global temperatures can materially reshape the equity–bond return trade-off. Three key results emerge. First, as temperatures rise and consumption growth weakens, the risk-free rate temporarily declines before converging back toward its long-run level once temperatures stabilize. Second, the equity risk premium rises because investors demand additional compensation for the long-horizon consumption risk induced by persistent warming. Calibrations to recent damage estimates and transition costs imply increases between 12% and 25% under a 3°C scenario. Third, allowing for temperature-linked volatility makes the premium explicitly state dependent, amplifying market sensitivity to climate conditions.

These findings underscore that even gradual, chronic warming —even absent sudden disasters— has first-order effects on expected returns and, consequently, on asset valuations and portfolio risk. They also highlight the value of reduced-form models in settings where historical data offer limited guidance for unprecedented climate trajectories. Future research could enrich this baseline by incorporating heterogeneous regional damages, feedback from policy responses and adaptation, or interactions with tipping point risks. Such extensions would further clarify how evolving climate dynamics shape the cost of capital and the stability of financial markets in a warming world.

The proposed model offers a robust and carefully calibrated framework that links long-run macroeconomic dynamics with a persistent climate and policy states, allowing for explicit scenario analysis of physical and transition risks. Its closed-form solutions for the risk-free rate and equity risk premium make it transparent and tractable, yet flexible enough to incorporate alternative damage estimates, transition costs, policy pathways, stochastic volatility in temperature dynamics, and asset-specific climate characteristics. This flexibility enables investors to evaluate portfolio exposure to warming scenarios and to stress-test

asset valuations under different climate trajectories. At the same time, the model provides regulators and policymakers with a quantitative tool for assessing systemic vulnerabilities in financial markets and for designing prudential measures—such as climate-related capital buffers or disclosure requirements—that reflect the scale and transmission channels of climate risk.

Appendix A Damage estimates

Damage functions produce diverging estimates of global GDP losses at future warming levels. Table 5 summarizes projected losses, measured relative to a counterfactual GDP trajectory, at 2 °C and 3 °C above pre-industrial levels across a selection of studies.

Study	**Impact at 2 °C global warming**[1] *(Current Policies in 2050*[2]*)*	**Impact at 3 °C global warming**[1] *(Current Policies in 2100*[2]*)*
Nordhaus and Boyer (2000)	1%	2%
Tol (2009)	1%	3%
Weitzman (2012)	1%	3%
Dell et al. (2012)	4%	22%
Tol (2014)	1%	2%
Nordhaus (2014)	1%	2%
Dietz and Stern (2015)	2%	13%
Burke et al. (2015)	8%	14%
Howard and Sterner (2017)	3%	8%
Kompas et al. (2018)	1%	2%
Kalkuhl and Wenz (2020)	2%	5%
Kahn et al. (2021)	3%	8%
Waidelich et al. (2024)	4%	8%
Bilal and Känzig (2024)	19%	44%
Kotz et al. (2024)	14%	33%

[1] Damage estimates relative to a baseline without further climate change. The percentages shown are based on harmonized calculations for cross-study comparability and may deviate from loss projections in the original studies. [2] Global warming projections according to Global Change Assessment Model (GCAM) 6.0 in Phase V of the NGFS Scenarios. Using RCP8.5, the most severe of the seven Representative Concentration Pathways (RCPs) presented in the IPCC's Fifth Assessment Report, global warming will reach 2.3 °C in its median estimate by mid-century. Even when using the 95$^{\text{th}}$ percentile of the temperature distribution of RCP8.5, global warming reaches 2.9 °C by 2050.

Table 5: **Damage estimates across studies.** *Source: NGFS (2024a), "Damage functions, NGFS scenarios, and the economic commitment of climate change."*

Appendix B Model derivations

We present the derivations for the general setup of five processes with stochastic volatility (for symmetry, all five processes are assumed to possibly record stochastic volatility)

$$\Delta c_{t+1} = \mu + x_t + \Omega Y_{t+1} + \Gamma(P_{t+1} - \bar{P}) + \sigma_\eta \sqrt{1 + \pi_\eta Y_t}\eta_{t+1} \tag{21}$$

$$x_{t+1} = \rho x_t + \sigma_\epsilon \sqrt{1 + \pi_\epsilon Y_t}\epsilon_{t+1} \tag{22}$$

$$Y_{t+1} = \beta Y_t + T_{t+1} - T_t + \sigma_\omega \sqrt{1 + \pi_\omega Y_t}\omega_{t+1} \tag{23}$$

$$T_{t+1} = \nu T_t + (1-\nu)P_t + \Theta x_t + \sigma_\zeta \sqrt{1 + \pi_\zeta Y_t}\zeta_{t+1} \tag{24}$$

$$P_{t+1} = \alpha P_t + (1-\alpha)\bar{P} + \sigma_\iota \sqrt{1 + \pi_\iota Y_t}\iota_{t+1} \tag{25}$$

B.1 Aggregate consumption and wealth process

The guess and verify price-to-wealth ratio

$$z_t^c = A_0^c + A_1^c x_t + A_2^c T_t + A_3^c Y_t + A_4^c P_t \tag{26}$$

The Campbell-Shiller approximation, based on ex-dividend wealth, writes as

$$r_{t+1}^c = \kappa_0^c + \Delta c_{t+1} + z_{t+1}^c - \kappa_1^c z_t^c, \tag{27}$$

$$\kappa_1^c = \frac{e^{\bar{z}^c}}{e^{\bar{z}^c} - 1}, \quad \kappa_0^c = \kappa_1^c \bar{z}^c - \ln(e^{\bar{z}^c} - 1), \tag{28}$$

$$\bar{z}^c = A_0^c + A_1^c \bar{x} + A_2^c \bar{T} + A_3^c \bar{Y} + A_4^c \bar{P}.$$

The stochastic discount factor and Euler equation, with $\theta = \frac{1-\gamma}{1-\frac{1}{\psi}}$ writes as

$$m_{t+1} = \theta \log \delta - \frac{\theta}{\psi}\Delta c_{t+1} + (\theta - 1) r_{t+1}^c \tag{29}$$

$$1 = \mathbf{E}_t[\exp(m_{t+1} + r_{t+1})] \tag{30}$$

Then, when recalling that for a normal process rv_{t+1}^N

$$\mathbf{E}_t[\exp(rv_{t+1}^N)] = \exp\left(\mathbf{E}_t[rv_{t+1}^N] + \frac{1}{2}\mathbf{V}_t[rv_{t+1}^N]\right)$$

the Euler equation applied to the wealth process writes as

$$\begin{aligned} 0 &= \theta \log \delta + \theta\kappa_0^c + \mathbf{E}_t[rv_{t+1}] + \frac{1}{2}\mathbf{V}_t[rv_{t+1}] \\ rv_{t+1} &= (1-\gamma)\Delta c_{t+1} + \theta[z_{t+1}^c - \kappa_1^c z_t^c] \end{aligned}$$

Identifying the x_t terms

$$\begin{aligned} 0 &= (1-\gamma) + \theta[\rho - \kappa_1^c]A_1 \\ A_1^c &= \frac{(1-1/\psi)(1+\Omega\Theta) + \Theta(A_2^c + A_3^c)}{\kappa_1^c - \rho} \end{aligned} \tag{31}$$

Identifying the T_t terms

$$\begin{aligned} 0 &= (1-\gamma)\Omega(\nu-1) + \theta[(\nu - \kappa_1^c)A_2^c + (\nu-1)A_3^c] \\ A_2^c &= \frac{(1-1/\psi)\Omega(\nu-1) + (\nu-1)A_3^c}{\kappa_1^c - \nu} \end{aligned} \tag{32}$$

Identifying the Y_t terms

$$\begin{aligned} 0 &= (1-\gamma)\beta\Omega + \theta(\beta - \kappa_1^c)A_3 + \frac{1}{2}V_2^{ec} \\ A_3^c &= \frac{(1-1/\psi)\beta\Omega + \frac{1}{2\theta}V_2^{ec}}{\kappa_1^c - \beta} \end{aligned} \tag{33}$$

$$\begin{aligned} V_2^{ec} &= \pi_\eta(\beta_\eta^c - \lambda_\eta)^2\sigma_\eta^2 + \pi_\epsilon(\beta_\epsilon^c - \lambda_\epsilon)^2\sigma_\epsilon^2 + \pi_\zeta(\beta_\zeta^c - \lambda_\zeta)^2\sigma_\zeta^2 \\ &\quad + \pi_\omega(\beta_\omega^c - \lambda_\omega)^2\sigma_\omega^2 + \pi_\iota(\beta_\iota^c - \lambda_\iota)^2\sigma_\iota^2 \end{aligned} \tag{34}$$

Identifying the P_t terms

$$\begin{aligned} 0 &= (1-\gamma)[\Omega(1-\nu)+\Gamma\alpha] + \theta[(1-\nu)A_2^c + (1-\nu)A_3^c + (\alpha-\kappa_1^c)A_4^c] \\ A_4^c &= \frac{(1-1/\psi)[\Omega(1-\nu)+\Gamma\alpha] + (1-\nu)(A_2^c + A_3^c)}{\kappa_1^c - \alpha} \end{aligned} \tag{35}$$

Identifying the intercept terms

$$\begin{aligned} 0 &= \theta\log\delta + (1-\gamma)[\mu - \Gamma\alpha\bar{P}] + \theta[\kappa_0^c + (1-\kappa_1^c)A_0^c + (1-\alpha)\bar{P}A_4] \\ &\quad + \frac{1}{2}\left[(1-\gamma)^2\sigma_\eta^2 + (\theta A_1^c)^2\sigma_\epsilon^2 + ((1-\gamma)\Omega + \theta A_2^c + \theta A_3^c)^2\sigma_\zeta^2 + ((1-\gamma)\Omega + \theta A_3^c)^2\sigma_\omega^2 + (\theta A_4^c)^2\sigma_\iota^2\right] \\ A_0^c &= \frac{\log\delta + \kappa_0^c + (1-1/\psi)[\mu - \Gamma\alpha\bar{P}] + (1-\alpha)\bar{P}A_4^c + \frac{1}{2\theta}V_1^{ec}}{\kappa_1^c - 1} \end{aligned} \tag{36}$$

where

$$V_1^{ec} = (\beta_\eta^c - \lambda_\eta)^2\sigma_\eta^2 + (\beta_\epsilon^c - \lambda_\epsilon)^2\sigma_\epsilon^2 + (\beta_\zeta^c - \lambda_\zeta)^2\sigma_\zeta^2 + (\beta_\omega^c - \lambda_\omega)^2\sigma_\omega^2 + (\beta_\iota^c - \lambda_\iota)^2\sigma_\iota^2 \tag{37}$$

$$\tag{38}$$

and the consumption process exposures are defined by

$$\beta_\eta^c = 1 \tag{39}$$

$$\beta_\epsilon^c = A_1^c \tag{40}$$

$$\beta_\zeta^c = A_2^c + A_3^c + \Omega \tag{41}$$

$$\beta_\omega^c = A_3^c + \Omega \tag{42}$$

$$\beta_\iota^c = A_4^c + \Gamma \tag{43}$$

$$\tag{44}$$

B.2 Risk-free rate

The stochastic discount factor writes as

$$m_{t+1} = \theta \log \delta + (\theta - 1)\kappa_0^c - \gamma \Delta c_{t+1} + (\theta - 1)[z_{t+1}^c - \kappa_1^c z_t^c]$$

so that

$$\begin{aligned} m_{t+1} - \mathbf{E}_t[m_{t+1}] = &-\lambda_\eta \sigma_\eta \sqrt{1 + \pi_\eta Y_t}\eta_{t+1} - \lambda_\zeta \sigma_\zeta \sqrt{1 + \pi_\zeta Y_t}\zeta_{t+1} - \lambda_\epsilon \sigma_\epsilon \sqrt{1 + \pi_\epsilon Y_t}\epsilon_{t+1} \\ &- \lambda_\omega \sigma_\omega \sqrt{1 + \pi_\omega Y_t}\omega_{t+1} - \lambda_\iota \sigma_\iota \sqrt{1 + \pi_\iota Y_t}\omega_{t+1} \end{aligned}$$

when we identify the five risk prices

$$\lambda_\eta = \gamma \tag{45}$$

$$\lambda_\epsilon = (1 - \theta)A_1^c \tag{46}$$

$$\lambda_\zeta = (1 - \theta)(A_2^c + A_3^c) + \gamma\Omega \tag{47}$$

$$\lambda_\omega = (1 - \theta)A_3^c + \gamma\Omega \tag{48}$$

$$\lambda_\iota = (1 - \theta)A_4^c + \gamma\Gamma \tag{49}$$

Eventually, the risk-free rate is defined as

$$r_{f,t} = -\ln \mathbf{E}_t[\exp(m_{t+1})].$$

Given the A^c's determined earlier, we derive the result of Proposition 1

$$r_{f,t} = r_f + \frac{1 + \Omega\Theta}{\psi}x_t + \frac{\Omega\beta}{\psi}Y_t + (1 - \nu)\frac{\Omega}{\psi}[P_t - T_t] + \alpha\frac{\Gamma}{\psi}[P_t - \bar{P}] + \left[\left(1 - \frac{1}{\theta}\right)\frac{V_2^{ec}}{2} - \frac{V_2^e}{2}\right]Y_t \tag{50}$$

$$r_f = -\log\delta + \frac{1}{\psi}\mu + \left(1 - \frac{1}{\theta}\right)\frac{V_1^{ec}}{2} - \frac{V_1^e}{2} \tag{51}$$

with the constant terms

$$V_1^e = \lambda_\eta^2\sigma_\eta^2 + \lambda_\epsilon^2\sigma_\epsilon^2 + \lambda_\zeta^2\sigma_\zeta^2 + \lambda_\omega^2\sigma_\omega^2 + \lambda_\iota^2\sigma_\iota^2 \tag{52}$$

$$V_2^e = \pi_\eta\lambda_\eta^2\sigma_\eta^2 + \pi_\epsilon\lambda_\epsilon^2\sigma_\epsilon^2 + \pi_\zeta\lambda_\zeta^2\sigma_\zeta^2 + \pi_\omega\lambda_\omega^2\sigma_\omega^2 + \pi_\iota\lambda_\iota^2\sigma_\iota^2 \tag{53}$$

B.3 Dividends

We posit a flexible form for the dividend process as suggested in Appendix G

$$\begin{aligned}\Delta d_{t+1} = {} & \varphi\Delta c_{t+1} + (1-\varphi)\Big[\mu + \Omega\hat{Y}_{t+1}\Big] \\ & + \chi_1\Omega T_{t+1} + \chi_2\Omega Y_{t+1} + \chi_3\Gamma(P_{t+1} - \bar{P}) + \sigma_u\sqrt{1+\pi_u Y_t}u_{t+1}\end{aligned} \tag{54}$$

with the deterministic processes $\hat{T}$ and $\hat{Y}$.

The guess-and-verify linear price-dividend ratio for the asset writes as

$$z_t^d = A_0^d + A_1^d x_t + A_2^d T_t + A_3^d Y_t + A_4^d P_t + A_5^d\hat{T}_t + A_6^d\hat{Y}_t. \tag{55}$$

The Campbell-Shiller approximation for the cum-dividend return r^d of the asset is such that

$$r_{t+1}^d = \kappa_0^d + \Delta d_{t+1} + \kappa_1^d z_{t+1}^d - z_t^d, \tag{56}$$

$$\kappa_1^d = \frac{e^{\bar{z}^d}}{e^{\bar{z}^d}+1}, \quad \kappa_0^d = \ln(e^{\bar{z}^d}+1) - \kappa_1^d\bar{z}^d, \tag{57}$$

$$\bar{z}^d = A_0^d + A_1^d\bar{x} + A_2^d\bar{T} + A_3^d\bar{Y} + A_4^d\bar{P} + A_5^d\bar{\hat{T}} + A_6^d\bar{\hat{Y}}.$$

The A^d's get identified from the Euler equation

$$1 = \mathbf{E}_t[\exp(m_{t+1} + r_{t+1}^d)],$$

which can be re-cast in a similar fashion as earlier as

$$0 = \theta \log \delta + (\theta - 1)\kappa_0^c + \kappa_0^d + (1-\varphi)\Big[\mu + \Omega(\beta \hat{Y}_t + (\nu - 1)[\hat{T}_t - \bar{P}])\Big] + \mathbf{E}_t[rv_{t+1}^d] + \frac{1}{2}\mathbf{V}_t[rv_{t+1}^d]$$

$$\begin{aligned} rv_{t+1}^d &= (\varphi - \gamma)\Delta c_{t+1} + \chi_1 \Omega T_{t+1} + \chi_2 \Omega Y_{t+1} + \chi_3 \Gamma(P_{t+1} - \bar{P}) \\ &\quad + (\theta - 1)[z_{t+1}^c - \kappa_1^c z_t^c] + \kappa_1^d z_{t+1}^d - z_t^d + \sigma_u \sqrt{1 + \pi_u Y_t} u_{t+1} \end{aligned}$$

Identifying the x_t terms

$$\begin{aligned} 0 &= (\varphi - \gamma) + (\theta - 1)[\rho - \kappa_1^c]A_1^c + [\rho \kappa_1^d - 1]A_1^d \\ A_1^d &= \frac{(\varphi - 1/\psi)(1 + \Omega\Theta) + \kappa_1^d \Theta(A_2^d + A_3^d)}{1 - \rho\kappa_1^d} \end{aligned} \tag{58}$$

Identifying the T_t terms

$$\begin{aligned} 0 &= (\varphi - \gamma)\Omega(\nu - 1) + \chi_1 \Omega \nu + \chi_2 \Omega + (\nu - 1) \\ &\quad + (\theta - 1)[(\nu - \kappa_1^c)A_2^c + (\nu - 1)A_3^c] + (\kappa_1^d \nu - 1)A_2^d + \kappa_1^d(\nu - 1)A_3^d \\ A_2^d &= \frac{(\varphi - 1/\psi)\Omega(\nu - 1) + \chi_1 \Omega \nu + \chi_2 \Omega(\nu - 1) + \kappa_1^d(\nu - 1)A_3^d}{1 - \nu\kappa_1^d} \end{aligned} \tag{59}$$

Identifying the Y_t terms

$$\begin{aligned} 0 &= (\varphi - \gamma)\Omega\beta + \chi_2 \Omega\beta + (\theta - 1)(\beta - \kappa_1^c)A_3^c + (\kappa_1^d \beta - 1)A_3^d + \frac{1}{2}V_2^{ed} \\ A_3^d &= \frac{(\varphi - 1/\psi)\Omega\beta + \chi_2 \Omega\beta - \frac{1}{2}\left(1 - \frac{1}{\theta}\right)V_2^{ec} + \frac{1}{2}V_2^{ed}}{1 - \beta\kappa_1^d} \end{aligned} \tag{60}$$

$$V_2^{ed} = \pi_\eta[\beta_\eta^d - \lambda_\eta]^2\sigma_\eta^2 + \pi_\epsilon[\beta_\epsilon^d - \lambda_\epsilon]^2\sigma_\epsilon^2 + \pi_\zeta[\beta_\zeta^d - \lambda_\zeta]^2\sigma_\zeta^2 + \pi_\omega[\beta_\omega^d - \lambda_\omega]^2\sigma_\omega^2 + \pi_\iota[\beta_\iota^d - \lambda_\iota]^2\sigma_\iota^2 + \pi_u\sigma_u^2 \tag{61}$$

Identifying the P_t terms

$$
\begin{aligned}
0 &= (\varphi-\gamma)[\Omega(1-\nu)+\Gamma\alpha]+(\chi_1\Omega+\chi_2\Omega)(1-\nu)+\chi_3\Gamma\alpha+(\theta-1)[(1-\nu)(A_2^c+A_3^c)+(\alpha-\kappa_1^c)A_4^c] \\
&\quad +\kappa_1^d(1-\nu)(A_2^d+A_3^d)+(\kappa_1^d\alpha-1)A_4^d \\
A_4^d &= \frac{(\varphi-1/\psi)[\Omega(1-\nu)+\Gamma\alpha]+(\chi_1+\chi_2)\Omega(1-\nu)+\chi_3\Gamma\alpha+\kappa_1^d(1-\nu)(A_2^d+A_3^d)}{1-\kappa_1^d\alpha}
\end{aligned} \tag{62}
$$

Identifying the $\hat{T}_t$ terms

$$
\begin{aligned}
0 &= (1-\varphi)\Omega(\nu-1)+\left[\kappa_1^d\nu-1\right]A_5^d+\kappa_1^d(\nu-1)A_6^d \\
A_5^d &= \frac{(1-\varphi)\Omega(\nu-1)+\kappa_1^d(\nu-1)A_6^d}{1-\nu\kappa_1^d}
\end{aligned} \tag{63}
$$

Identifying the $\hat{Y}_t$ terms

$$
\begin{aligned}
0 &= (1-\varphi)\Omega\beta+\left[\kappa_1^d\beta-1\right]A_6^d \\
A_6^d &= \frac{(1-\varphi)\Omega\beta}{1-\beta\kappa_1^d}
\end{aligned} \tag{64}
$$

Identifying the intercept terms

$$
\begin{aligned}
0 &= \theta\log\delta+\kappa_0^d+(1-\gamma)[\mu-\Gamma\alpha\bar{P}]-\chi_3\Gamma\alpha\bar{P}+(1-\varphi)\Omega(1-\nu)\bar{P}+\kappa_1^d(1-\nu)(A_5^d+A_6^d)\bar{P} \\
&\quad +(\theta-1)[\kappa_0^c+(1-\kappa_1^c)A_0^c+(1-\alpha)\bar{P}A_4^c]+(\kappa_1^d-1)A_0^d+\kappa_1^d(1-\alpha)\bar{P}A_4^d+\frac{1}{2}V_1^{ed}
\end{aligned}
$$

Let's define the dividend process exposures

$$\beta_\eta^d = \varphi \tag{65}$$

$$\beta_\epsilon^d = \kappa_1^d A_1^d \tag{66}$$

$$\beta_\zeta^d = \kappa_1^d (A_2^d + A_3^d) + \varphi\Omega + \chi_1\Omega \tag{67}$$

$$\beta_\omega^d = \kappa_1^d A_3^d + \varphi\Omega + \chi_2\Omega \tag{68}$$

$$\beta_\iota^d = \kappa_1^d A_4^d + \varphi\Gamma + \chi_3\Gamma \tag{69}$$

and

$$V_1^{ed} = [\beta_\eta^d - \lambda_\eta]^2\sigma_\eta^2 + [\beta_\zeta^d - \lambda_\zeta]^2\sigma_\zeta^2 + [\beta_\epsilon^d - \lambda_\epsilon]^2\sigma_\epsilon^2 + [\beta_\omega^d - \lambda_\omega]^2\sigma_\omega^2 + [\beta_\iota^d - \lambda_\iota]^2\sigma_\iota^2 + \sigma_u^2 \tag{70}$$

So that the coefficient simplifies out as

$$A_0^d = \frac{\log\delta + (1-1/\psi)\mu - (\varphi - 1/\psi)\Gamma\alpha\bar{P} + (1-\varphi)\Omega(1-\nu)\bar{P} + a_0^d - \frac{1}{2}\left(1-\frac{1}{\theta}\right)V_1^{ec} + \frac{1}{2}V_1^{ed}}{1-\kappa_1^d} \tag{71}$$

$$a_0^d = \kappa_0^d + \kappa_1^d(1-\alpha)\bar{P}A_4^d + \kappa_1^d(1-\nu)(A_5^d + A_6^d)\bar{P} - \chi_3\Gamma\alpha\bar{P}$$

Eventually, the returns on the dividend process can be expressed and simplified as

$$\begin{aligned}
r_{t+1}^d &= \kappa_0^d + \Delta d_{t+1} + \kappa_1^d z_{t+1}^d - z_t^d \\
&= -\log\delta + \frac{1}{\psi}\mu + \frac{1+\Omega\Theta}{\psi}x_t + \frac{\Omega\beta}{\psi}Y_t + (1-\nu)\frac{\Omega}{\psi}[P_t - T_t] + \alpha\frac{\Gamma}{\psi}[P_t - \bar{P}] \\
&+ \left(1-\frac{1}{\theta}\right)\frac{V_1^{ec}}{2} - \frac{V_1^{ed}}{2} + \left[\left(1-\frac{1}{\theta}\right)\frac{V_2^{ec}}{2} - \frac{V_2^{ed}}{2}\right]Y_t \\
&+ \beta_\eta^d\sigma_\eta\sqrt{1+\pi_\eta Y_t}\eta_{t+1} + \beta_\zeta^d\sigma_\zeta\sqrt{1+\pi_\zeta Y_t}\zeta_{t+1} + \beta_\epsilon^d\sigma_\epsilon\sqrt{1+\pi_\epsilon Y_t}\epsilon_{t+1} \\
&+ \beta_\omega^d\sigma_\omega\sqrt{1+\pi_\omega Y_t}\omega_{t+1} + \beta_\iota^d\sigma_\iota\sqrt{1+\pi_\iota Y_t}\iota_{t+1} + \sigma_u\sqrt{1+\pi_u Y_t}u_{t+1}
\end{aligned}$$

and in turn

$$\ln \mathbf{E}_t[\exp(r^d_{t+1})] = -\log\delta + \frac{1}{\psi}\mu + \frac{1+\Omega\Theta}{\psi}x_t + \frac{\Omega\beta}{\psi}Y_t + (1-\nu)\frac{\Omega}{\psi}[P_t - T_t] + \alpha\frac{\Gamma}{\psi}[P_t - \bar{P}] + \left(1-\frac{1}{\theta}\right)\frac{V_1^{ec}}{2} - \frac{V_1^{ed}}{2} + \frac{V_1^d}{2} + \left[\left(1-\frac{1}{\theta}\right)\frac{V_2^{ec}}{2} - \frac{V_2^{ed}}{2} + \frac{V_2^d}{2}\right]Y_t$$

when defining the constant terms

$$V_1^d = (\beta_\eta^d)^2\sigma_\eta^2 + (\beta_\epsilon^d)^2\sigma_\epsilon^2 + (\beta_\zeta^d)^2\sigma_\zeta^2 + (\beta_\omega^d)^2\sigma_\omega^2 + (\beta_\iota^d)^2\sigma_\iota^2 + \sigma_u^2 \tag{72}$$

$$V_2^d = \pi_\eta(\beta_\eta^d)^2\sigma_\eta^2 + \pi_\epsilon(\beta_\epsilon^d)^2\sigma_\epsilon^2 + \pi_\zeta(\beta_\zeta^d)^2\sigma_\zeta^2 + \pi_\omega(\beta_\omega^d)^2\sigma_\omega^2 + \pi_\iota(\beta_\iota^d)^2\sigma_\iota^2 + \pi_u\sigma_u^2 \tag{73}$$

Eventually, the equity risk premium from Propositions 2 is

$$\begin{aligned} ERP_t^d &= \ln \mathbf{E}_t[\exp(r^d_{t+1})] - r_{f,t} \\ &= \frac{1}{2}\left(V_1^e + V_1^d - V_1^{ed} + \left[V_2^e + V_2^d - V_2^{ed}\right]Y_t\right) \\ &= \beta_\eta^d\lambda_\eta\sigma_\eta^2 + \beta_\zeta^d\lambda_\zeta\sigma_\zeta^2 + \beta_\epsilon^d\lambda_\epsilon\sigma_\epsilon^2 + \beta_\omega^d\lambda_\omega\sigma_\omega^2 + \beta_\iota^d\lambda_\iota\sigma_\iota^2 \\ &+ \left[\pi_\eta\beta_\eta^d\lambda_\eta\sigma_\eta^2 + \pi_\epsilon\beta_\epsilon^d\lambda_\epsilon\sigma_\epsilon^2 + \pi_\zeta\beta_\zeta^d\lambda_\zeta\sigma_\zeta^2 + \pi_\omega\beta_\omega^d\lambda_\omega\sigma_\omega^2 + \pi_\iota\beta_\iota^d\lambda_\iota\sigma_\iota^2\right]Y_t \end{aligned} \tag{74}$$

Appendix C Proof of signs

We work under the assumption that the preference parameters are $\gamma > 1$ and $\psi > 1$ so that $\theta < 0$. The damage and transition coefficients are $\Omega < 0$ and $\Gamma < 0$. The economic to temperature impact parameter $\Theta > 0$. We also focus on the case where $\chi_1 = \chi_2 = \chi_3 = 0$ Also, from their definitions in 28 and 57,respectively, $\kappa_1^c > 1$ and $\kappa_1^d < 1$

C.1 Short-run risk

The signs of short-run and long-run risk coefficients, price of risk, and exposures are straightforward.

On the short-run front, these variables are all single positive coefficients, so that $\lambda_\eta > 0$, $\beta_\eta^c > 0$, $\beta_\eta^d > 0$.

C.2 Temperature risks

First, focusing on temperature change from 33 and 60 we can conclude that $A_3^c < 0$ and $A_3^d < 0$ in all cases when stochastic volatility is off. In turn the price of risk $\lambda_\omega < 0$, and the exposures $\beta_\omega^c < 0$, $\beta_\omega^d < 0$. All these negative signs are nuanced when stochastic volatility is incorporated.

Second, when still staying clear of stochastic volatility, from 32 and 59 we can conclude that $A_2^c > 0$ and $A_2^d > 0$. Then, we can identify the regularity conditions that let $A_2^c + A_3^c < 0$ and similarly $A_2^d + A_3^d < 0$. From 32 and 33, the regularity condition is $(1 - 1/\psi)\Omega(\nu - 1) + (\kappa_1^c - 1)A_3^c + \frac{1}{2\theta}V_2^{ec} < 0$ and simplifies out to $\frac{\kappa_1^c - 1}{\kappa_1^c - \beta}\beta < 1 - \nu$. This condition is numerically verified. In turn we can conclude that the temperature level price of risk is negative $\lambda_\zeta < 0$, and so are the exposures $\beta_\zeta^c < 0$, $\beta_\zeta^d < 0$.

C.3 Long-run risk

On the long-run front, from 31, without economic impact on temperature we would conclude immediately that $A_1^c > 0$, and in turn $\lambda_\epsilon > 0$ and $\beta_\epsilon^c > 0$. From 58 we would conclude that $A_1^d > 0$, and in turn $\beta_\epsilon^d > 0$. However, the econo-temperature interplay mutes the long-run risk key coefficients A_1^c and A_1^d via two channels: the direct damage channel via $\Omega\Theta < 0$, and the secondary channel via $\Theta(A_2^c + A_3^c)$, and symmetrically $\Theta(A_2^d + A_3^d)$, which are also negative under the previous regularity condition.

C.4 Policy risk

Policy risks are facing multiple cross-currents. They inherit from the damage risk stemming from temperature, while directly capturing transition risks.

First, leaving aside both stochastic volatility and transition risks, the previous condition would let us conclude from 35 that $A_4^c < 0$. In turn $\lambda_\iota < 0$ and $\beta_\iota^c < 0$, $\beta_\iota^d < 0$.

These signs are all counteracted by transition risk, and depending on the strength of the relative factors, may flip entirely. We eventually notice an intriguing knife-edge case, if $\gamma < \phi$, and Γ is small enough that $\lambda_\iota < 0$, one may concommittantly observe $\beta_\iota^d > 0$.

Appendix D Table of calibrated parameters

Process	Parameter	Notation	Value
Preferences			
	time impatience	δ	0.998
	relative risk aversion	γ	10
	elasticity of intertemporal substitution	ψ	1.5
Consumption			
	equilibrium consumption growth	μ_c	0.0015
	volatility of the short-run risk	σ_η	0.0078
	volatility of the long-run risk	σ_ϵ	0.00034
	persistence of the long-run risk	ρ	0.979
Temperature			
	initial temperature	T_0	1.25°C
	persistence of the temperature	ν	0.999
	volatility of the temperature risk	σ_ζ	0.033
Temperature change			
	persistence of the signal	β	0.962
	volatility of the signal	σ_w	0.02
Policy			
	initial policy temperature	P_0	4°C
	long-run target temperature	$\bar{P}$	4°C
	persistence of the policy	α	0.9999
	volatility of the policy risk	σ_i	0.045
Feedbacks			
	damage coefficient	Ω	-0.0102
	transition coefficient	Γ	0.0004
	economic impact on temperature	Θ	0.2
Stochastic volatility			
	stochastic volatility of the short-run risk	π_η	2.96
	stochastic volatility of the long-run risk	π_ϵ	0.00
Dividends			
	dividend leverage	φ	2.5
	volatility of the dividend risk	σ_u	0.00

Table 6: **Calibrated model parameters.** Simulations are performed on monthly time steps. We generate 100000 paths.

Appendix E Calibration

E.1 Climate module

The climate module captures the salient features of climate physics. It is calibrated so that certain percentiles of its distributional paths replicate benchmark climate scenarios.

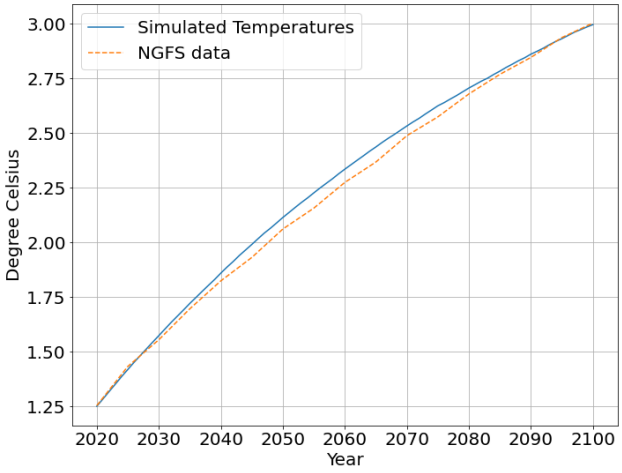

Figure 7: **Calibration of ν parameter.** Trajectory of global temperature anomaly in NGFS Current Policy scenario and mean estimate across the temperature paths in our climate module.

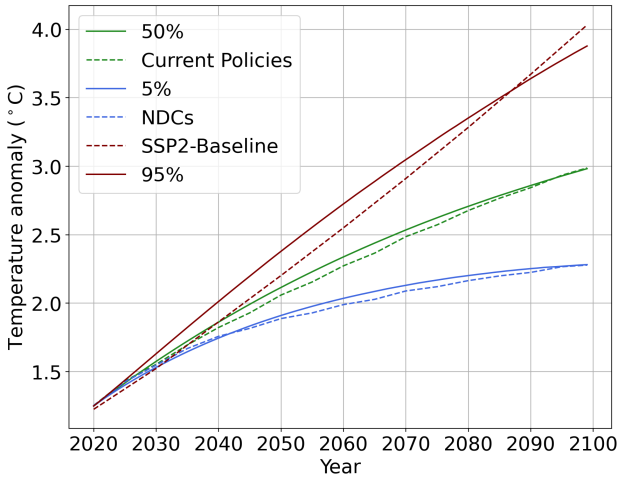

Figure 8: **Calibration of σ_ι parameter.** Percentiles of temperatures in our climate module versus NGFS scenarios. $\nu = 0.99895$, $\alpha = 0.9999$, $\sigma_\zeta = 0$, $\sigma_\iota = 0.045$, $P_0 = \bar{P} = 4$.

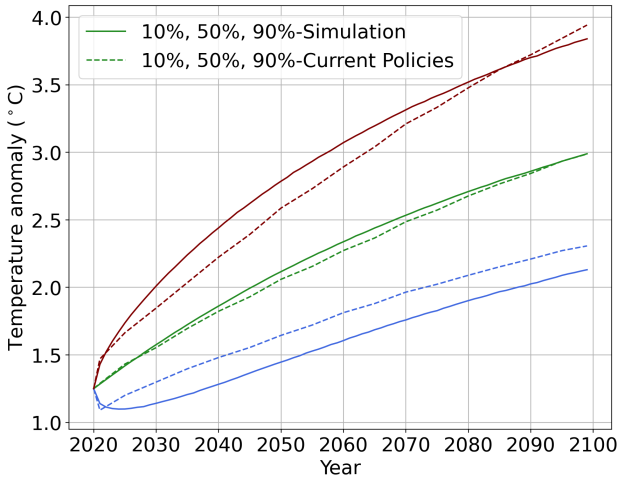

Figure 9: **Calibration of σ_ζ parameter.** Percentiles of temperatures in our climate module versus NGFS scenarios. $\nu = 0.99895$, $\alpha = 0.9999$, $\sigma_\zeta = 0.033$, $\sigma_\iota = 0.0$, $P_0 = \bar{P} = 4$. Solid lines represent simulation quantiles, Dashed lines represent NFGS *Current Policies* quantiles.

E.2 Vanishing temperature change process

Figure 10 illustrates the calibration of the persistence of the Y_t process. The Y_t process converges to zero in all three cases in the chart because the impact of the initial temperature shock is not permanent. With $\beta = 0.96$, the impact of the initial shock is almost zero after 120 months. With a higher $\beta = 0.99$, 30% of the initial shock remains in the system after 120 months, representing a more persistent impact.

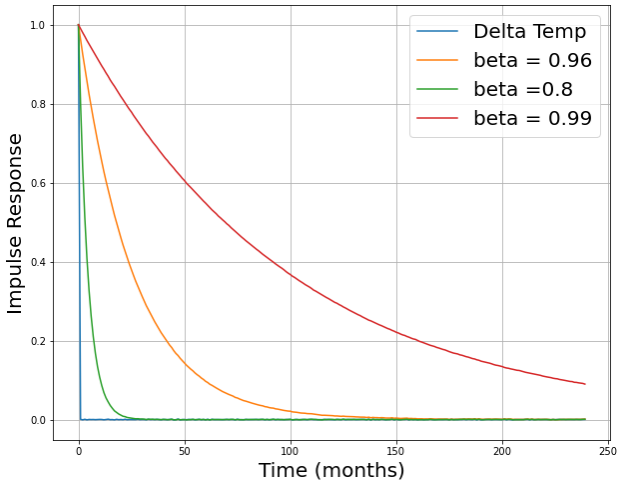

Figure 10: **Temperature change memory persistence.** Suppose the temperature jumps by 1°C at the beginning and then stays constant (the blue line). The green, orange and red lines illustrate the dynamics of the Y_t process with different βs.

Figure 11 illustrates the calibration of the volatility parameter σ_ω which is fitted to replicate at the 5th and 95th percentile of the Y_t process distribution the profile of longer (15-year) and shorter (5-year) memory processes than the 10-year memory used as benchmark.

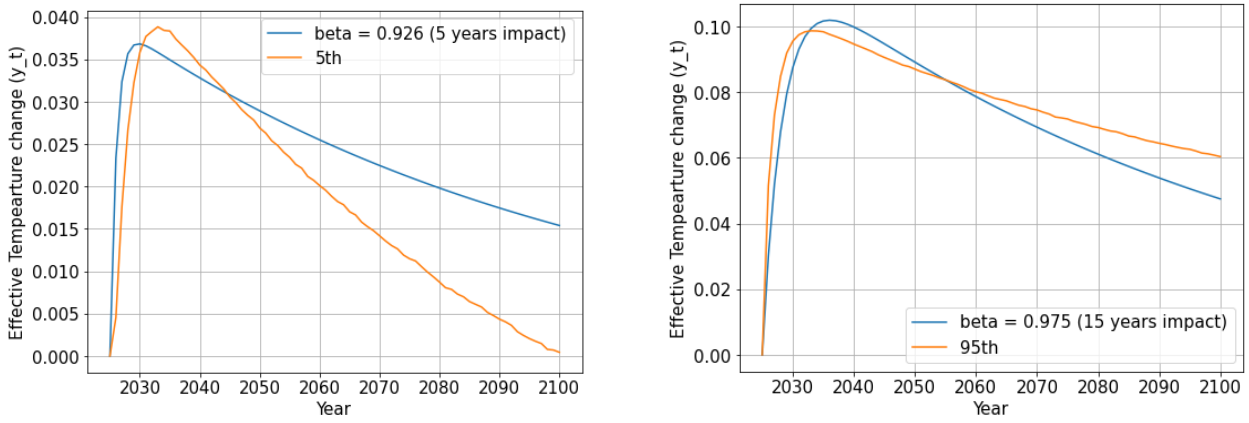

Figure 11: **Calibration of σ_ω parameter.** Percentiles of temperatures in our climate module versus model with varied β corresponding to 5-year and 15-year memory.

E.3 Calibration of damages

Figure 12 illustrates the expected consumption under the two damage scenarios in comparison with the counterfactual consumption. The expected consumption growth in the counterfactual case is assumed to be 1.8% per year, similar to the assumed annual GDP growth in the SSP2 scenario, which is also the counterfactual GDP growth rate used by the NGFS scenarios. With this growth rate, the expected consumption by 2100 will be 4.5 times higher than today's level. Under the "Low Damage" scenario, the expected consumption by 2100 is about 3 times higher than today's level, implying a loss of 33%. Under the "High Damage" scenario, the consumption loss increases to 44%.

The expected consumption growth also falls due to the impact of the rising temperatures. In particular, it falls significantly during the rapid warming period. However, the drop in consumption growth is not permanent. As temperature stabilizes, the impact of

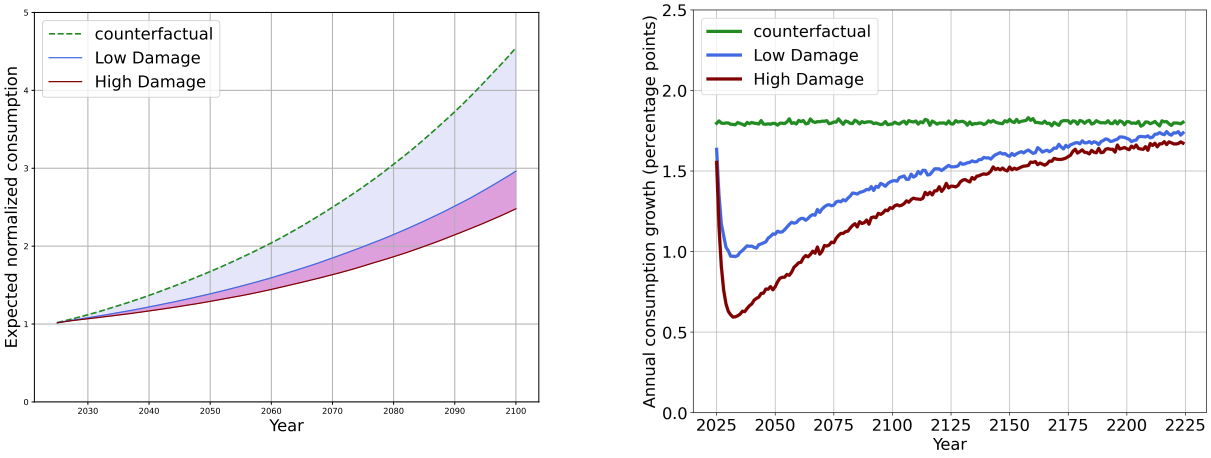

Figure 12: **Expected consumption under two damage scenarios and counterfactual.** Mean trajectory of consumption in levels (LHS) and representative path for consumption growth (RHS).

rising temperature gradually fades, and the consumption growth will converge back to the counterfactual level in a long horizon; see Figure 12 for an illustration.

E.4 Calibration of transition costs

Figure 13 presents the profiles of transition costs, denominated as % of GDP loss compared to the counterfactual, of key NGFS scenarios. The "Net zero 2050" scenario losses are used to calibrate our Γ parameter.

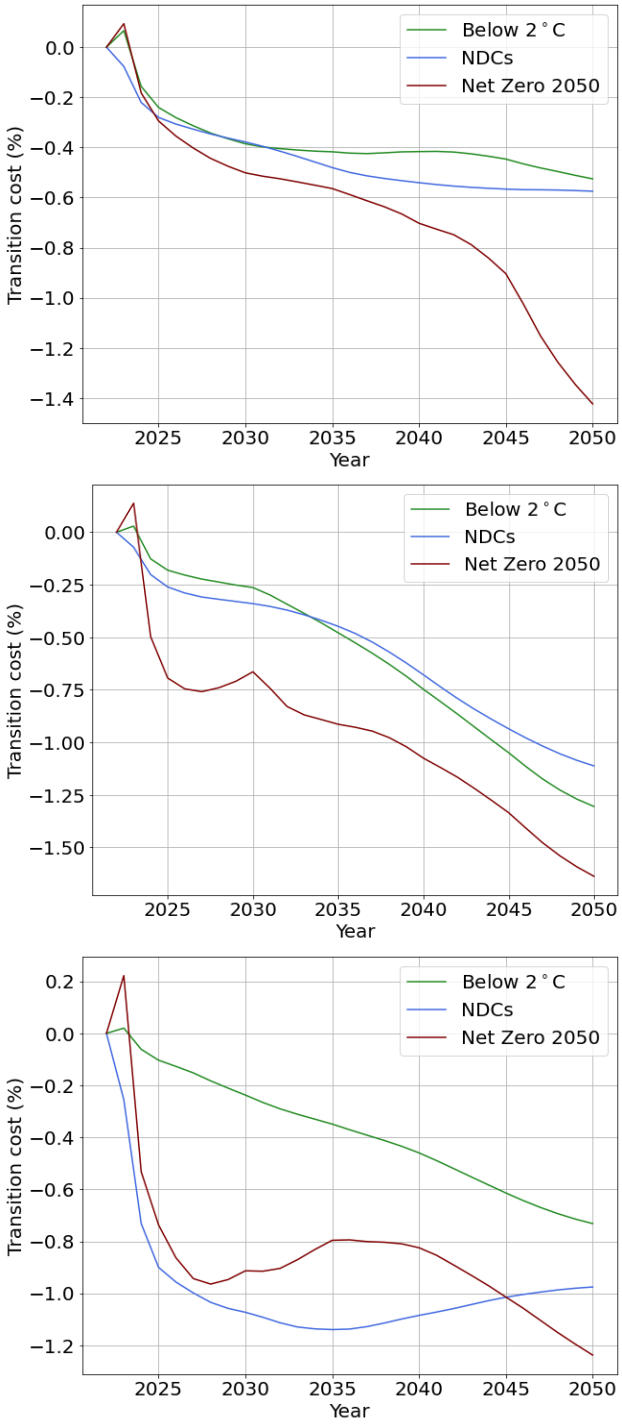

Figure 13: **Transition under different NGFS scenarios.** Plots in following order: GCAM, Message and Remind. World figures.

E.5 Calibration of economic impact on temperature

Table 7 presents the average growth rates recorded along the five shared socioeconomic pathways envisioned by the IPCC.

	SSP1	SSP2	SSP3	SSP4	SSP5
Average annual growth rate	2.02%	1.99%	1.15%	1.44%	2.75%

Table 7: **Average global GDP growth rates between 2025 and 2100**

Figure 14 presents the quantiles of temperature pathways in the situation where x_t is permanently adding 1 percentage point of growth to our framework. Our Θ parameter is calibrated so that a temperature of 5°C by the end of the century, typically considered in the climate literature as a temperature level that could start jeopardizing human life on Earth, is recorded in the last percentile of the temperature distribution.

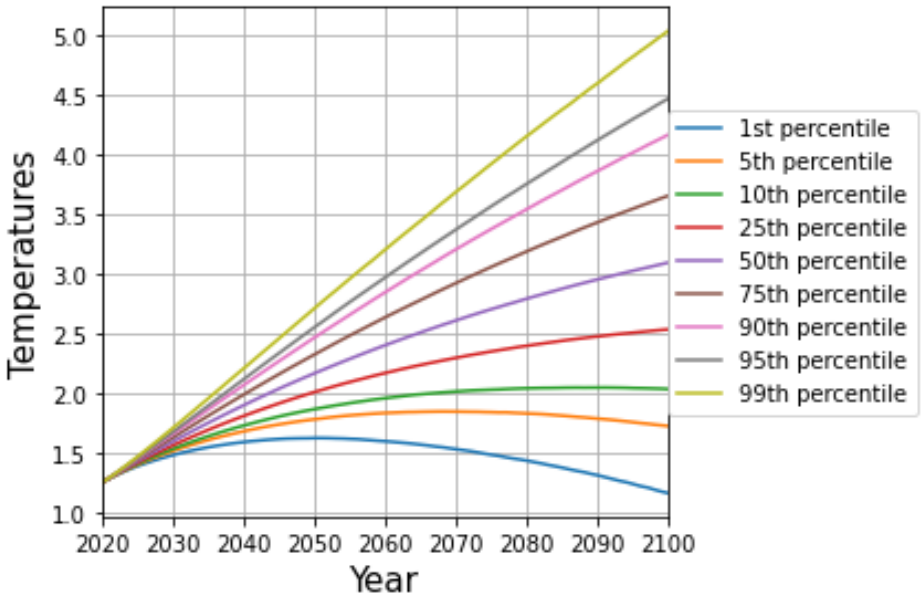

Figure 14: **Calibration of economic activity impact on temperatures.** Simulation parameters: $\Theta = 0.2$, $\rho = 1$, $x_0 = 0.01/12$, $\sigma_\zeta = 0$ and $\sigma_\iota = 0$.

Appendix F Supplementary numerical results

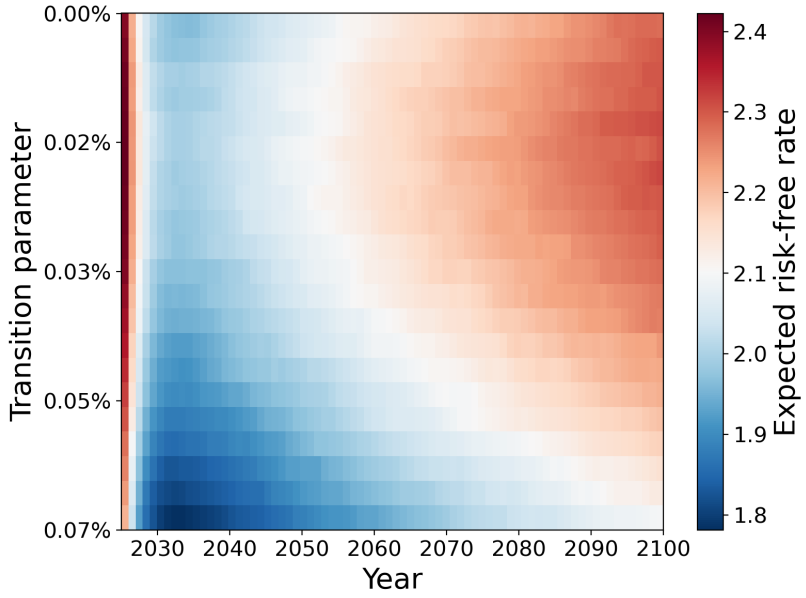

Figure 15: **Risk-free rate time-profile for different transition costs.** Parameters: $\Omega = -0.0102, \Theta = 0.2, \pi_\eta = 0$ varying Γ.

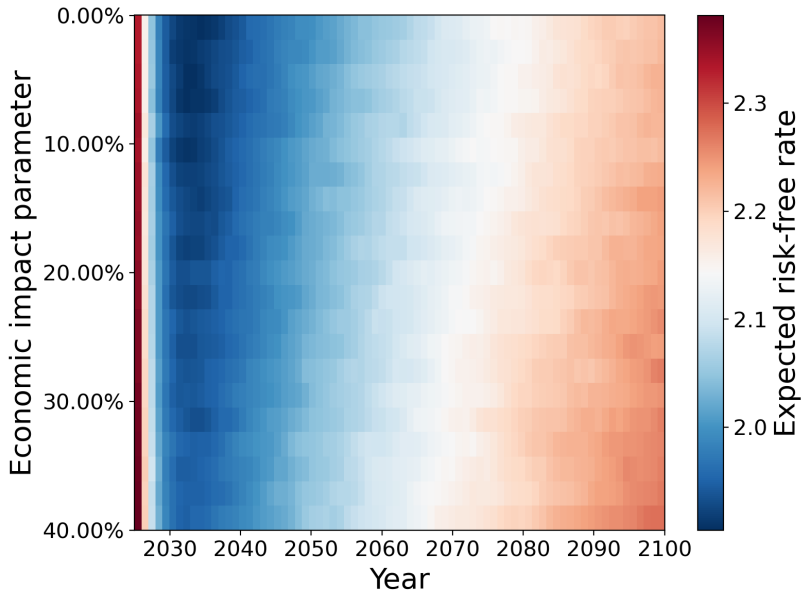

Figure 16: **Risk-free rate time-profile for different strengths of economic impact to temperature.** Parameters: $\Omega = -0.0102, \Gamma = 0.00045, \pi_\eta = 0$ varying Θ.

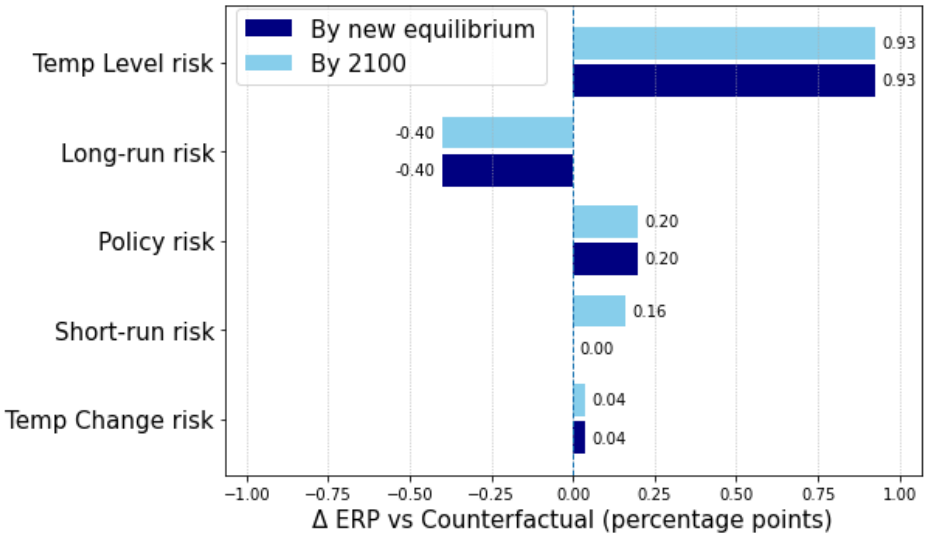

Figure 17: **ERPs with climate vs counterfactual.** Five components.

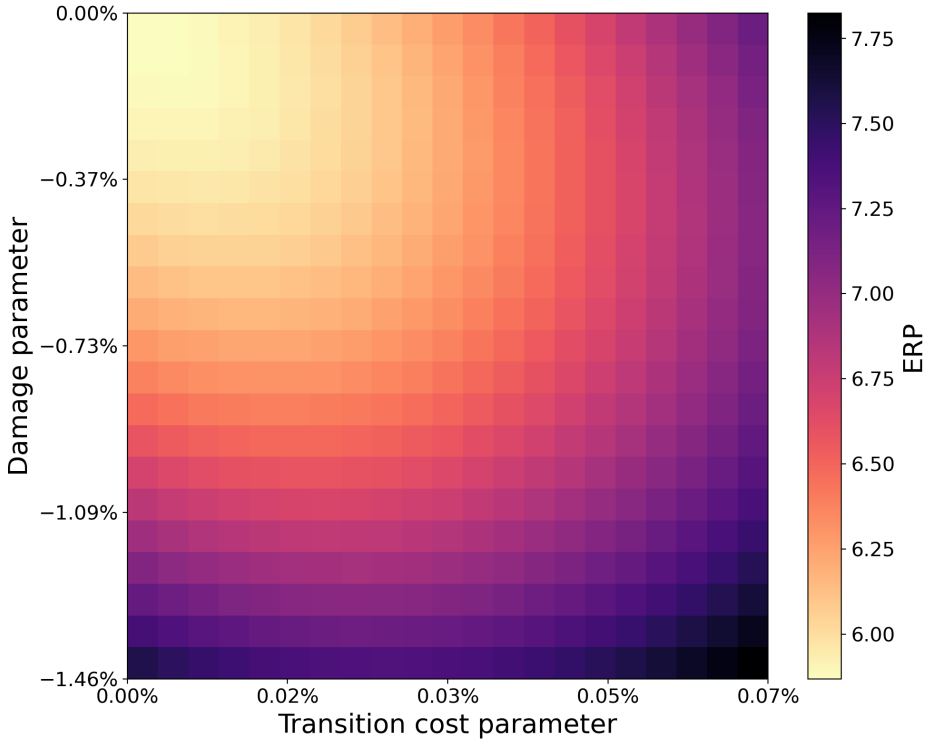

Figure 18: **ERP sensitivity to transition and damage risks**. Heatmap response of equilibrium ERP to varying Ω and Γ parameters.

Appendix G Dividends' specific exposure to physical and transition risk

Our modeling framework accommodates a variety of dividend processes. While the simple leverage-consumption paradigm is suited to model global equity, it falls short in capturing sectoral, geographical or idiosyncratic patterns. The setup extends naturally to express the fact that certain assets may be more (or less) exposed to physical, transition or stranding risk than the global equity market

$$\Delta d_{t+1} = \varphi \Delta c_{t+1} + (1-\varphi)\Big[\mu + \Omega \hat{Y}_{t+1}\Big] + \chi_1 \Omega T_{t+1} + \chi_2 \Omega Y_{t+1} + \chi_3 \Gamma (P_{t+1} - \bar{P}) + \sigma_{u,t} u_{t+1}. \tag{75}$$

Structurally, the exposures of the dividend process reflect the additional components. Letting the standard notations relate to the dividend process described in Equation (75), two exposures from Lemma 2 are impacted:

1. The exposure to the temperature level risk is now $\beta_\zeta^d = \kappa_1^d (A_2^d + A_3^d) + \varphi\Omega + \chi_1 \Omega$;
2. The exposure to the temperature change risk is now $\beta_w^d = \kappa_1^d A_3^d + \varphi\Omega + \chi_2 \Omega$;
3. The exposure to the policy risk is now $\beta_\iota^d = \kappa_1^d A_4^d + \varphi\Gamma + \chi_3 \Gamma$.

References

Addoum, J. M., Ng, D. T., and Ortiz-Bobea, A. (2020). Temperature Shocks and Establishment Sales. *The Review of Financial Studies*, 33(3):1331–1366.

Addoum, J. M., Ng, D. T., and Ortiz-Bobea, A. (2023). Temperature shocks and industry earnings news. *Journal of Financial Economics*, 150(1):1–45.

Baldauf, M., Garlappi, L., and Yannelis, C. (2020). Does Climate Change Affect Real Estate Prices? Only If You Believe In It. *The Review of Financial Studies*, 33(3):1256–1295.

Bansal, R., Dittmar, R. F., and Lundblad, C. T. (2005). Consumption, Dividends, and the Cross Section of Equity Returns. *The Journal of Finance*, 60(4):1639–1672.

Bansal, R., Kiku, D., and Ochoa, M. (2016). Climate Change and Growth Risks. *NBER working paper*.

Bansal, R., Kiku, D., and Ochoa, M. (2019). Climate Change Risk. In *Climate Change Economics: The Role of Uncertainty and Risk*. Edited by V V. Chari and Robert Litterman.

Bansal, R., Kiku, D., and Yaron, A. (2011). An Empirical Evaluation of the Long-Run Risks Model for Asset Prices. *Critical Finance Review*, 1(1):183–221.

Bansal, R. and Yaron, A. (2004). Risks for the Long Run: A Potential Resolution of Asset Pricing Puzzles. *The Journal of Finance*, 59(4):1481–1509.

Barnett, M., Brock, W., and Hansen, L. P. (2020). Pricing Uncertainty Induced by Climate Change. *The Review of Financial Studies*, 33(3):1024–1066.

Beeler, J. and Campbell, J. Y. (2011). The Long-Run Risks Model and Aggregate Asset Prices: An Empirical Assessment. *Critical Finance Review*, 1(1):141–182.

Bernstein, A., Gustafson, M. T., and Lewis, R. (2019). Disaster on the horizon: The price effect of sea level rise. *Journal of financial economics*, 134(2):253–272.

Bilal, A. and Känzig, D. R. (2024). The Macroeconomic Impact of Climate Change: Global vs. Local Temperature. *NBER working paper*.

Bua, G., Kapp, D., Ramella, F., and Rognone, L. (2024). Transition versus physical climate risk pricing in european financial markets: A text-based approach. *The European Journal of Finance*, 30(17):2076–2110.

Burke, M., Hsiang, S. M., and Miguel, E. (2015). Global Non-Linear Effect of Temperature on Economic Production. *Nature*, 527(7577):235–239.

DeFries, R. S., Edenhofer, O., Halliday, A. N., Heal, G. M., Lenton, T., Puma, M., Rising, J., Rockström, J., Ruane, A., Schellnhuber, H. J., Stainforth, D., Stern, N., Tedesco, M., and Ward, B. (2019). The missing economic risks in assessments of climate change impacts. *Policy Insight The Earth Institute Columbia University*.

Dell, M., Jones, B. F., and Olken, B. A. (2012). Temperature Shocks and Economic Growth: Evidence from the Last Half Century. *American Economic Journal: Macroeconomics*, 4(3):66–95.

Dietz, S. and Stern, N. (2015). Endogenous Growth, Convexity of Damage and Climate Risk: How Nordhaus' Framework Supports Deep Cuts in Carbon Emissions. *The Economic Journal*, 125(583):574–620.

Engle, R. F., Giglio, S., Kelly, B., Lee, H., and Stroebel, J. (2020). Hedging Climate Change News. *The Review of Financial Studies*, 33(3):1184–1216.

Epstein, L. G. and Zin, S. E. (1989). Substitution, Risk Aversion, and the Temporal Behavior of Consumption and Asset Returns: A Theoretical Framework. *Econometrica*, 57(4):937–969.

Geoffroy, O., Saint-Martin, D., Bellon, G., Voldoire, A., Olivié, D. J., and Tytéca, S. (2013a). Transient climate response in a two-layer energy-balance model. part ii: Representation

of the efficacy of deep-ocean heat uptake and validation for cmip5 aogcms. *Journal of Climate*, 26(6):1859–1876.

Geoffroy, O., Saint-Martin, D., Olivié, D. J., Voldoire, A., Bellon, G., and Tytéca, S. (2013b). Transient climate response in a two-layer energy-balance model. part i: Analytical solution and parameter calibration using cmip5 aogcm experiments. *Journal of climate*, 26(6):1841–1857.

Giglio, S., Kelly, B., and Stroebel, J. (2021). Climate Finance. *Annual Review of Financial Economics*, 13(1):15–36.

Gostlow, G. (2024). Anything Goes: Pricing Physical Climate Risk. *Working Paper*.

Hong, H. G., Li, F. W., and Xu, J. (2021). Climate Risks and Market Efficiency. *Journal of Econometrics*.

Howard, P. H. and Sterner, T. (2017). Few and Not So Far Between: A Meta-analysis of Climate Damage Estimates. *Environmental and Resource Economics*, 68(1):197–225.

Kahn, M. E., Mohaddes, K., Ng, R. N. C., Pesaran, M. H., Raissi, M., and Yang, J.-C. (2021). Long-term macroeconomic effects of climate change: A cross-country analysis. *Energy Economics*, 104:105624.

Kalkuhl, M. and Wenz, L. (2020). The impact of climate conditions on economic production. Evidence from a global panel of regions. *Journal of Environmental Economics and Management*, 103:102360.

Kompas, T., Pham, V. H., and Che, T. N. (2018). The Effects of Climate Change on GDP by Country and the Global Economic Gains From Complying With the Paris Climate Accord. *Earth's Future*, 6(8):1153–1173.

Kotz, M., Levermann, A., and Wenz, L. (2024). The economic commitment of climate change. *Nature*, 628(8008):551–557.

Leach, N. J., Jenkins, S., Nicholls, Z., Smith, C. J., Lynch, J., Cain, M., Walsh, T., Wu, B., Tsutsui, J., and Allen, M. R. (2021). Fairv2. 0.0: a generalized impulse response model for climate uncertainty and future scenario exploration. *Geoscientific Model Development*, 14(5):3007–3036.

Nath, I. B., Ramey, V. A., and Klenow, P. J. (2024). How Much Will Global Warming Cool Global Growth? *NBER working paper*.

NGFS (2024a). Damage functions, NGFS scenarios, and the economic commitment of climate change. *Network for Greening the Financial System Working Paper*.

NGFS (2024b). Ngfs long-term scenarios for central banks and supervisors. Technical report, Network for Greening the Financial System.

Nordhaus, W. (2014). Estimates of the Social Cost of Carbon: Concepts and Results from the DICE-2013R Model and Alternative Approaches. *Journal of the Association of Environmental and Resource Economists*, 1(1/2):273–312.

Nordhaus, W. D. and Boyer, J. (2000). *Warming the World*. The MIT Press.

Painter, M. (2020). An inconvenient cost: The effects of climate change on municipal bonds. *Journal of Financial Economics*, 135(2):468–482.

Pástor, L., Stambaugh, R. F., and Taylor, L. A. (2021). Sustainable investing in equilibrium. *Journal of Financial Economics*, 142(2):550–571.

Tol, R. S. J. (2009). The Economic Effects of Climate Change. *Journal of Economic Perspectives*, 23(2):29–51.

Tol, R. S. J. (2014). Correction and Update: The Economic Effects of Climate Change. *Journal of Economic Perspectives*, 28(2):221–226.

Tsutsui, J. and Smith, C. (2024). Revisiting two-layer energy balance models for climate assessment. *Environmental Research Letters*, 20(1):014059.

Waidelich, P., Batibeniz, F., Rising, J., Kikstra, J. S., and Seneviratne, S. I. (2024). Climate damage projections beyond annual temperature. *Nature Climate Change*, 14(6):592–599.

Weil, P. (1989). The equity premium puzzle and the risk-free rate puzzle. *Journal of Monetary Economics*, 24(3):401–421.

Weitzman, M. L. (2012). GHG Targets as Insurance Against Catastrophic Climate Damages. *Journal of Public Economic Theory*, 14(2):221–244.

Zhang, S. Y. (2022). Are investors sensitive to climate-related transition and physical risks? evidence from global stock markets. *Research in International Business and Finance*, 62:101710.